

Reply to the interactive comment on “Wavelet analysis of the singular spectral reconstructed time series to study the imprints of solar-ENSO-Geomagnetic activity on Indian climate’ by S. Sri Lakshmi and R.K.Tiwari

Referee #1

The authors are very much thankful to the reviewer for his professional comments and suggestions for improving the manuscript. We have incorporated the reviewer’s suggestions accordingly:

(i) *In particular, the comment regarding the phrase "highlights the removal of noise in the data" in the conclusion and coordinates from where the data of WH have been taken from (the authors claim they added this information to the caption of Figure 1, however, I cannot find it there).*

As suggested by the reviewer, we have modified the phrase as “The application of wavelet analysis for the SSA reconstructed time series, along with the removal of noise in the data identifies the existence of a high-amplitude, recurrent, multi-decadal scale patterns that are present in Indian temperature records”.

The coordinates from where the data of WH have been taken are from mean pre-monsoon temperature anomalies for AD 1226–2000 (Yadav et. al., 2004) where we have selected the time period from 1876-2000 for our present work.

(ii) *Additional comment is regarding the statement of the problem in at the end of Introduction: lines 107-109. The objective of the manuscript is not clear. Maybe re-formulated as "using wavelet analysis to find the".*

As the reviewer has suggested, we have modified the sentence as “Here our main objective is to employ wavelet-based analysis on SSA reconstructed time series to find out the evidence of the possible linkages, if any, among ENSO–solar-geomagnetic in the Indian temperature records”

Technical comments:-

1. Could you please remove "most" in line 59?

The word “most” has been removed.

- 2. Could the authors please clarify the sentence of lines 78-79? Regarding: contributions of.. to...**

The sentence in lines 78-79 has been modified accordingly as suggested by the reviewer.

- 3. "Availability of data is very less" can be reformulated as "there is a lack of data"**

The sentence in lines 89-90 has been modified accordingly as suggested by the reviewer.

- 4. Line 92: "In recent years" can be omitted.**

The word "In recent years" has been omitted.

- 5. Line 101: after citation please add 'we'**

The word 'we' has been added after the citation.

- 6. I would recommend using "reveal" instead of "gain" in line 103**

The word 'reveal' was written instead of "gain".

- 7. Line 128: please add "available" after the "Himalayas"**

The word "available" was added after the "Himalayas".

- 8. Line 138: Just "methods" , without applied.**

The word "applied" has been removed.

- 9. "Climatic structure" is mentioned in line 138, but explained later, in line 149.**

The word "Climatic structure" has been removed to avoid confusion in the manuscript.

- 10. Line 150. The first sentence can be removed.**

The first sentence can be removed.

- 11. Please be consistent with formulas' format in the text.**

The formulas are thoroughly checked once again in the text.

- 12. Please spell out AMO in line 298. I assume, it is Atlantic Meridional Oscillation, but it would be easier for the reader. Also, the result regarding AMO is not reflected in the conclusion of the manuscript. I believe the manuscript would benefit from adding a sentence about AMO to the conclusion.**

The word AMO was spelled out in line 295 as suggested by the reviewer and also a sentence on Atlantic Multi-decadal Oscillation was added in the conclusion.

- 13. Could the authors please provide a reference for the study of solar modulation and ENSO?**

References on the study of solar modulation and ENSO have been added in the lines (334 & 376) of the manuscript.

14. Please remove "&" and spell it out in line 407.

The symbol "&" was removed and also spelled out in line 406.

Reviewer 2:

The authors are very much thankful to the reviewer for his comments and suggestions for improving the manuscript. We have incorporated the reviewer's suggestions accordingly:

1. Line 17: "The other" -> "Other"

The word "The other" was replaced by "Other".

2. Line 19: "span" -> "period"

The word "span" was replaced by "period".

3. Line 20: "to" -> "and of the"

The word "span" was replaced by "period".

4. Line 22: "in tree" -> "in the tree"

The word "in tree" was replaced by "in the tree".

5. Line 24: "wavelet" -> "a wavelet"

The word "wavelet" was replaced by "a wavelet".

6. Add "activity" after "solar-geomagnetic"

The word "activity" was added after "solar-geomagnetic".

7. Line 28: "atmosphere" -> "atmospheric"

The word "atmosphere" was replaced by "atmospheric".

8. Line 28: "on" -> "on the"

The word "on" was replaced by "on the".

9. Line 31: " Indian" -> "the Indian"

The word "Indian" was replaced by "the Indian".

10. Line 34: "suggest" -> "suggest the"

The word "suggest" was replaced by "suggest the".

11. Line 50: "affects" -> "effects"

The word "affects" was replaced by "effects".

12. Line 62: Add "the" before "atmosphere" and "global"

The word "the" was added before "atmosphere" and "global".

13. Line 85: Add "a" before "possibility"

The word "a" was added before "possibility".

14. Line 92: Add "a" before "promising"

The word “a” was added before “promising”.

15. Line 99: "in" -> "on"

The word “in” was replaced by “on”.

16. Line 101: "In" -> "In a"

The word “In” was replaced by “In a”.

17. Line 106: What is the meaning of "Troup"

The method used by the Australian Bureau of Meteorology is the Troup SOI which is the standardised anomaly of the Mean Sea Level Pressure difference between Tahiti and Darwin. (<http://www.bom.gov.au/climate/glossary/soi.shtml>)

18. Line 115: "a common" -> "the common"

The word “a common” was replaced by “the common”.

19. Line 133: What is the meaning of "chorological"?

The word “chorological” was replaced by “chronological”.

20. Line 136: Remove "(Figure 1)"

The word “(Figure 1)” was removed.

21. Line 147: "independent" -> "uncorrelated"

The word “independent” was replaced by “uncorrelated” in line 146

22. Line 154: "lag-corrections" -> "lag-correlations"

The word “lag-corrections” was corrected “lag-correlations” in line 152-153.

23. Line 173: Di needs subscript i

The subscript was placed properly.

24. Line 178&180: Ti subscript i

The subscript was placed properly.

25. Line 183: Which equation?

The equation (3) was addressed properly.

26. Line 187: "intital" -> "initial"

The word “intital” was replaced by “initial”.

27. Line 310: Why is it nonstationary?

The time series is considered here to be non-stationary because the series remains to be time-variant and the observed spectral peaks (power) split in the interval of 2- 8 years.

28. Line 348: "slowing" -> "slowly"

The word “slowing” was replaced by “slowly”.

29. Line 368: "in sense" -> "in the sense"

The word "in sense" was replaced by "in the sense".

1 **WAVELET ANALYSIS OF THE SINGULAR SPECTRAL RECONSTRUCTED TIME SERIES TO STUDY**
2 **THE IMPRINTS OF SOLAR-ENSO-GEOMAGNETIC ACTIVITY ON INDIAN CLIMATE**

3
4 **¹S. Sri Lakshmi* and ²R. K. Tiwari**

5
6 ¹ University Centre for Earth and Space Sciences, University of Hyderabad, Hyderabad 500 046,
7 India

8 ² CSIR-National Geophysical Research Institute, Uppal Road, Hyderabad 500 007, India

9
10 ***Corresponding Author:** srilakshmi.uceess@gmail.com
11 Tel.: +91-40-23132671 (Office)
12 Fax: +91-40-23010152
13

14 **ABSTRACT**

15 To study the imprints of the Solar-ENSO-Geomagnetic activity on the Indian Subcontinent, we
16 have applied the Singular spectral analysis (SSA) and wavelet analysis to the tree ring
17 temperature variability record from the Western Himalayas. ~~Other~~~~The other~~ data used in the
18 present study are the Solar Sunspot Number (SSN), Geomagnetic Indices (aa Index) and
19 Southern Oscillation Index (SOI) for the common time ~~periodspan~~ of 1876-2000. Both SSA and
20 wavelet spectral analyses reveal the presence of 5-7 years short term ENSO variations and
21 ~~the~~ 11 year solar cycle indicating the possible combined influences of solar-geomagnetic
22 activities and ENSO -on the Indian temperature. Another prominent signal corresponding to 33-
23 year periodicity in the tree ring record suggests the Sun-temperature variability link probably
24 induced by changes in the basic state of the earth's atmosphere. In order to complement the
25 above findings, we performed a wavelet analysis of SSA reconstructed time series, which agrees
26 well with our earlier results and also increases the signals to noise ratio thereby showing strong
27 influence of solar-geomagnetic activity & ENSO throughout the entire -time period. The solar
28 flares are considered to be responsible for causing the ~~atmospheric~~~~atmosphere~~ circulation
29 patterns. The net effect of solar-geomagnetic processes on the temperature record might
30 suggest counteracting influences on shorter (about 5–6 y) and longer (about 11–12 y) time
31 scales. The present analyses suggest that the influence of solar activities on the Indian
32 temperature variability operates in part indirectly through coupling of ENSO on multilateral

33 time scales. The analyses, hence, provide credible evidence for tele-connections of tropical
34 pacific climatic variability and Indian climate ranging from inter-annual-decadal time scales and
35 also suggest the possible role of exogenic triggering in reorganizing the global earth-ocean-
36 atmospheric systems.

37 **Key words: Geomagnetic activity, Western Himalayas, Sunspot Number, SOI index, Singular**
38 **spectral analysis, Wavelet spectrum, Coherency.**

39

40 **1. Introduction:**

41 Several recent studies of solar/geomagnetic effects on climate have been examined on both
42 global as well as on regional scales (Lean and Rind, 2008; Benestaed and Schmidt, 2009; Meehl,
43 2009; Kiladis and Diaz 1989; Pant and Rupa Kumar 1997; Gray et al. 1992; Wiles et al. 1998; Friis
44 and Svensmark 1997; Rigozo et al. 2005; Feng et al. 2003; Tiwari and srilakshmi 2009; Chowdary
45 et al. 2006, 2014; Appenzeller et al. 1998; Proctor et al. 2002; Tsonis et al. 2005; Freitas and
46 Mclean 2013). The Sun's long-term magnetic variability caused by the sunspots is considered as
47 one of the primary drivers of climatic changes. The short-term magnetic variability is due to the
48 disturbances in Earth's magnetic fields caused by the solar activities and is indicated by the
49 geomagnetic indices. The Sun's magnetic variability modulates the magnetic and particulate
50 fluxes in the heliosphere. This determines the interplanetary conditions and imposes significant
51 electromagnetic forces and effectsaffects upon the planetary atmosphere. All these effects are
52 due to the changing solar-magnetic fields, which are relevant for planetary climates including
53 the climate of the Earth. The Sun-Earth relationship varies on different time scales ranging from
54 days to years bringing a drastic influence on the climatic patterns. The ultimate cause of solar
55 variability, at time scales from decadal to centennial to millennial or even longer scales has its
56 origin in the solar dynamo mechanism. During the solar maxima, huge amounts of solar energy
57 particles are released, thereby causing the geomagnetic disturbances. The 11 years solar cycle
58 acts as an important driving force for variations in the space weather, ultimately giving rise to
59 climatic changes. It is, therefore, imperative to understand the origin of space climate by
60 analyzing the different proxies of solar magnetic variabilities. Another most—important
61 phenomenonphenomena is El Nino-Southern Oscillation (ENSO), which produces droughts,

62 floods and intense rainfall. The strong coupling and interactions between the Tropical Ocean
63 and the atmosphere play a major role in the development of the global climatic system. The El
64 Nino events generally recur approximately every 3-5 years with large events spaced around 3-7
65 years apart. The ENSO phenomena have shown huge impact on the Asian monsoon (Cole et al.,
66 1993), Indian monsoon (Chowdary et al. 2006, 2014) as well as globally (Horel and Wallace
67 1981; Barnett 1989; Yasunari 1985; Nicholson 1997). In particular, the El Nino, solar,
68 geomagnetic activities are the major affecting forces on the decadal and interdecadal
69 temperature variability on global and regional scales in a direct/indirect way (El-Borie et al.
70 2010; ~~(Gray et al., 2010)~~. Recent studies (Frohlich and Lean 2004; Steinhilber et al. 2009)
71 indicate the possible influence of solar activity on Earth's temperature/climate on multi-decadal
72 time scales. The 11 year solar cyclic variations observed from the several temperature climate
73 records also suggest the impact of solar irradiance variability on terrestrial temperature
74 (Budyko 1969; Friis and Lassen 1991; Friis and Svensmark 1997; Kasatkina et al. 2007). The bi-
75 decadal (22 years) called the Hale cycle, is related to the reversal of the solar magnetic field
76 direction (Lean et al. 1995; Kasatkina et al. 2007). The 33 year cycle (Bruckener cycle) is also
77 caused by the solar origin, but it is a very rare cycle (Kasatkina et al. 2007). The 2–7 years ENSO
78 cyclic pattern and its possible coupling process is the major driving force for the temperature
79 variability (Gray et al. 1992; Wiles et al. 1998; Mokhov et al. 2000; Rigozo et al. 2007, Kothawale
80 et al. 2010). ~~El-BorieEl-Borie et al, 2010 have indicated the possible contributions for both the~~
81 ~~solar and geomagnetic indices. El-Borie and Al-Thoyaib, 2006; El-Borie et al., 2007 and El-Borie~~
82 ~~et al, 2010a, 2007~~ have indicated in their studies that the global temperature should lag the
83 geomagnetic activity with a maximum correlation when the temperature lags by 6 years.
84 Mendoza et. al., 1991 reported on possible connections between solar activity and El Nino's,
85 while Reid and Gage (1988) and Reid (1991) reported on the similarities between the 11-year
86 running means of monthly sunspot numbers and global sea surface temperature. These findings
87 suggest that there is a possibility of strong coupling between temperature-ENSO and solar-
88 geomagnetic signals.

89 The mean global temperature of the Earth's surface also plays a very important role in
90 bringing climatic changes. Several studies have been carried out to understand the detailed

91 climatic changes of India in the past millennium using various proxy records e.g. ice cores, lake
92 | sediments, glacier fluctuations, peat deposits etc. ~~There is a lack-availability~~ of high-precision
93 and high-resolution palaeo-climatic information for longer time scale from the Indian
94 | subcontinent. ~~Tree-ring is very less. In recent years, tree-ring~~ data is a promising proxy to
95 retrieve high resolution past climatic changes from several geographical regions of India
96 (Bhattacharyya et al. 1988; Bhattacharyya et al. 1992; Hughes, 1992; Bhattacharyya and Yadav,
97 1996; Borgaonkar et al. 1996; Chaudhary et al. 1999; Yadav et al. 1999; Bhattacharyya and
98 Chaudhary, 2003; Bhattacharyya et al. 2006; Shah et al. 200) It has been noted that tree-ring
99 based climatic reconstructions in India generally do not exceed beyond 400 years records
100 except at some sites in the Northwest Himalaya. Thus, a long record of tree-ring data is needed
101 | to extend available climate reconstruction further back to determine climatic variability ~~on~~
102 sub-decadal, decadal and century scale. However, ~~non-~~availability of older living trees in most
103 of the sites is hindering the preparation of long tree chronology. In a previous study (Tiwari and
104 Srilakshmi, 2009), we have studied the periodicities and non-stationary modes in the tree ring
105 temperature data from the same region (AD 1200-2000). To ~~reveal~~gain significant connections
106 among the Solar-geomagnetic-ENSO 'triad' phenomena on tree ring width in detail for the ~~time~~
107 period from 1876-2000, we have applied here the Singular spectral analysis (SSA) and the
108 wavelet spectral analysis for Sunspot data, geomagnetic data (aa index), Troup Southern
109 | Oscillation Index (SOI) and the Western Himalayas tree ring data. ~~Here our~~Our main objective
110 ~~here~~ is to ~~employ~~present a wavelet-based analysis ~~on~~of SSA reconstructed time series to ~~find~~
111 ~~out focus on~~ the evidence of the possible linkages, if any, among ENSO-solar-geomagnetic
112 ~~connections in the Indian temperature records, comparison to ENSO-geomagnetic and solar-~~
113 ~~ENSO connections.~~

Formatted: Font color: Red

115 2. Source and Nature of Data:

116 The data analyzed here includes the time series of (1) Smoothed Sunspot number for solar
117 activity (2) Geomagnetic activity data (aa indices) (3) Troup Southern Oscillation Index (SOI) for
118 the study of El Nino-Southern Oscillation called ENSO (4) Western Himalayan temperature
119 | variability record. All the data sets have been analyzed for the common period of 125 years

120 spanning over 1876-2000. The monthly sunspot number data has been obtained from the
121 Sunspot Index Data Center [http:// astro.oma.be/SIDC/](http://astro.oma.be/SIDC/). The Troup SOI data is obtained from the
122 Bureau of Meteorology of Australia, <http://www.bom.gov.au/climate/>. The data for
123 geomagnetic activity, aa Index, was provided by the National Geophysical Data Center, NGDC,
124 (<http://www.ngdc.noaa.gov/stp/GEOMAG/aastar.shtml>). The aa index is a measure of
125 disturbances level of Earth's magnetic field based on magnetometer observations at two, nearly
126 antipodal, stations in Australia and England. In recent studies, the tree ring proxy climate
127 indicators have been potentially used for extracting information regarding past seasonal
128 temperature or precipitation/drought based on the measurements of annual ring width. The
129 detailed description of the data has been presented elsewhere (Yadav et. al., 2004). A brief
130 account of the data pertinent to the present analysis, however, is summarized here. The tree
131 ring data being analyzed here is one of the best temperature variability records (1876 to 2000)
132 of the pre-monsoon season in the Western Himalayas [available](#). The mean temperature series
133 is obtained from nine weather stations including both from high and low elevation areas in the
134 Western Himalayas. Temperature variability history is based on widely spread pure Himalayan
135 cedar (*Cedrus deodara* (Roxb.) G. Don) trees and characterizes all the sites with almost no
136 ground vegetation and thereby minimizes individual variation in tree-ring sequences induced by
137 inter tree competition (Yadav et. al., 2004). The mean ~~chronological~~ [chronological](#) structure is
138 based on in total 60 radii from 45 trees, statistical feature of which show that the chronology is
139 suitable for dendro-climatic studies back to AD 1226 (Yadav et. al., 2004).

140 ~~(Figure-1)~~
141

142 **3. Methods applied:** To analyze the temporal series and to find the climatic structure, we have
143 here ~~applied~~ three methods: Principal component analysis (PCA), Singular Spectral analysis
144 (SSA) and wavelet analysis.

145 **3.1. Principal component analysis (PCA):** As a preliminary analysis, we have applied the
146 Principle component analysis (PCA) to the data sets to extract the principle components. PCA
147 technique is applied for the reduction and extraction for dimensionality of the data and to rate
148 the amount of variation present in the original data set. The purpose to apply the PCA is to

149 identify patterns in the given time series. The new components thereby obtained by the PCA
150 analysis are termed as PC1, PC2, PC3 and so on, (for the first, second and third principal
151 components) are ~~uncorrelated independent~~ and decrease the amount of variance from the
152 original data set. PC1 (the first component) captures most of the variance; PC2 captures the
153 second most of the variance and so on. ~~These components are treated as climatic factors or~~
154 ~~climatic structures.~~

Formatted: Font: +Body, 12 pt, Font color: Text 1

155 **3.2. Singular spectral analysis:** The Singular Spectrum Analysis (SSA) ~~method was developed as~~
156 ~~the new time series method since 1970s. This~~ method is designed to extract as much
157 information as possible from a short, noisy time series without any prior knowledge about the
158 dynamics underlying the series (Broomhead and King, 1986; Vautard and Ghil, [1989](#); [Alonso et al., 2005](#); [Golyandina et al., 2001](#)); ~~1989~~). The method is a form of principal component analysis
159 (PCA) applied to ~~lag-correlations lag-corrections~~ structures of the time series. The basic SSA
160 decomposes an original time series into a new series which consists of trend, periodic or quasi-

Formatted: Font: +Body, Font color: Text 1

Formatted: Font: (Default) +Body, Font color: Text 1

161 periodic and white noises according to the singular value decomposition (SVD) and provides the
162 reconstructed components (RCs). The basic steps involved in SSA are: decomposition (involves
163 embedding, singular value decomposition (SVD)) and reconstruction (involves grouping and
164 diagonal averaging). Embedding decomposes the original time series into the trajectory matrix;
165 SVD turns the trajectory matrix into the decomposed trajectory matrices. The reconstruction
166 stage involves grouping to make subgroups of the decomposed trajectory matrices and
167 diagonal averaging to reconstruct the new time series from the subgroups.

Formatted: Font: (Default) +Body, Font color: Text 1

Formatted: Font: (Default) +Body, Font color: Text 1

169 **Step1: Decomposition:**

170 **(a) Embedding:** The first step in the basic SSA algorithm is the embedding step where
171 the initial time series change into the trajectory matrix. Let the time series be $Y = \{y_1, \dots, y_N\}$
172 of length N without any missing values. Here the window length L is chosen such that $2 < L <$
173 $N/2$ to embed the initial time series. We map the time series Y into the L lagged vectors, $Y_i =$

174 $\{y_i, \dots, y_{i+L-1}\}$ for $i = 1, \dots, K$, where $K = N - L + 1$. The trajectory matrix T_Y ($L \times K$ dimensions) is

175 written as: $T_Y = \begin{pmatrix} Y_1 \\ Y_2 \\ \vdots \\ Y_K \end{pmatrix} \dots\dots\dots(1)$

176 **(b) Singular Value Decomposition (SVD):** Here we apply SVD to the trajectory matrix T_Y
 177 to decompose and obtain $T_Y = UDV'$ called eigentriples; where U_i ($K \times L$ dimensions; $1 < i < L$) is an
 178 orthonormal matrix; D_i ($1 < i < L$) is a diagonal matrix of order L ; V_i ($L \times L$ dimensions; $1 < i < L$) is
 179 a square orthonormal matrix.

Formatted: Subscript

180 The trajectory matrix is thus written as $T_Y = \sum_{i=1}^d U_i \sqrt{\lambda_i} V_i^T$;(2)

181 where the i^{th} Eigen triple of $T_i = U_i \times \sqrt{\lambda_i} \times V_i^T$, $i = 1, 2, 3, \dots, d$ in which $d = \max(i: \sqrt{\lambda_i} > 0)$.

182 **Step 2: Reconstruction:**

183 **(c) Grouping:** Here the matrix T_i is decomposed into subgroups according to the trend,
 184 periodic or quasi-periodic components and white noises. The grouping step of the
 185 reconstruction stage corresponds to the splitting of the elementary matrices T_i into several
 186 groups and summing the matrices within each group. Let $I = \{i_1, i_2, \dots, i_p\}$ be the group of indices
 187 i_1, \dots, i_p . Then the matrix T_I corresponding to the group I is defines as $T_I = T_{i_1} + T_{i_2} + \dots + T_{i_p}$. The split of
 188 the set of indices $J = 1, 2, \dots, d$ into the disjoint subsets I_1, I_2, \dots, I_m corresponds to the equation

Formatted: Subscript

Formatted: Subscript

189 (3):

190 $T = T_{I_1} + T_{I_2} + \dots + T_{I_m}$(3)

191 The sets I_1, \dots, I_m are called the eigen triple grouping.

192 **(d) Diagonal averaging:** The diagonal averaging transfers each matrix T into a time
 193 series, which is an additive component of the ~~initial~~ time series Y . If z_{ij} stands for a
 194 element matrix Z , the k th term of the resulting series is obtained by averaging z_{ij} over all i, j
 195 such that $i+j=k+2$. This is called diagonal averaging or the Hankelization of the matrix Z . The
 196 Hankel matrix HZ , is the trajectory matrix corresponding to the series obtained by the result of
 197 diagonal averaging.

198 Considering equation (3), let X ($L \times K$) matrix with elements x_{ij} , where $1 \leq i \leq L$, $1 \leq j \leq K$.
 199 Here diagonal averaging transforms matrix X to a series g_0, \dots, g_{T-1} using the formula:

$$g_k = \begin{cases} \frac{1}{k+1} \sum_{m=1}^{k+1} x_{m,k-m+2}^* & 0 \leq k < L^* - 1 \\ \frac{1}{L^*} \sum_{m=1}^{L^*} x_{m,k-m+2}^* & L^* - 1 \leq k < K^* \\ \frac{1}{T-k} \sum_{m=k-k^*+2}^{N-k+1} x_{m,k-m+2}^* & K^* - 1 \leq k < T \end{cases} \quad (4)$$

201 This diagonal averaging by equation (4) applied to the resultant matrix X_{in} , produces time series
 202 Y_n of length T . For such signal characteristics, it is essential to examine the time-frequency
 203 pattern as to understand whether a particular frequency is temporally consistent or
 204 inconsistent. Hence for non-stationary signals, we need a transform that will be useful to obtain
 205 the frequency content of the time series/signal as a function of time.

206 An alternative method for studying the non-stationarity of the time series is wavelet
 207 transform. For non-stationary signals, wavelets decomposition would be the most appropriate
 208 method because the analyzing functions (the wavelets function) are localized both in time and
 209 frequency.

210
 211 **3.3. Wavelet spectral analysis:** During the past decades, wavelet analysis has become a popular
 212 method for the analysis of aperiodic and quasi-periodic data (Grinsted et. al., 2004; Jevrejeva
 213 et. al., 2003; Torrence and Compo, 1998; Torrence and Webster, 1999). In particular, it has
 214 become an important tool for studying localized variations of power within a time series. By
 215 decomposing a time series into time-frequency space, the dominant modes of variability and
 216 their variation with respect to time can be identified. The wavelet transform has various
 217 applications in geophysics, including tropical convection (Weng and Lau 1994), the El Niño–
 218 Southern Oscillation (Gu and Philander 1995), etc. We have applied the wavelet analysis to
 219 analyze the non-stationary signals which permits the identification of main periodicities of
 220 ENSO-sunspot-geomagnetic in the time series. The results give us more insight information
 221 about the evolution of these variables in frequency-time mode.

222 A wavelet transform requires the choice of analyzing function Ψ (called “mother
 223 wavelet”) that has the specific property of time-frequency localization. The continuous wavelet
 224 transform revolves around decomposing the time series into scaling components for identifying
 225 oscillations occurring at fast (time) scale and other at slow scales. Mathematically, the
 226 continuous wavelets transform of a time series $f(t)$ can be given as:

227
$$W_{\psi}(f)(a, b) = \frac{1}{\sqrt{a}} \int_{-\infty}^{\infty} f(t) \psi\left(\frac{t-b}{a}\right) dt \dots\dots\dots(5)$$

228 Here $f(t)$ represents time series, Ψ is the base wavelets function (here we have chosen the
 229 Morlet function), with length that is much shorter than the time series $f(t)$. W stands for
 230 wavelet coefficients. The variable ‘ a ’ is called the scaling parameter that determines the
 231 frequency (or scale) so that varying ‘ a ’ gives rise to wavelet spectrum. The factor ‘ b ’ is related to
 232 the shift of the analysis window in time so that varying b represents the sliding method of the
 233 wavelet over $f(t)$.

234 In several recent analyses, complex Morlet wavelet has been found useful for
 235 geophysical time series analysis. The Morlet is mostly used to find out areas where there is high
 236 amplitude at certain frequencies. The complex Morlet wavelet can be represented by a periodic
 237 sinusoidal function with a Gaussian envelope and is excellent for Morlet wavelet may be
 238 defined mathematically, as follows:

239
$$\psi(t) = \pi^{-1/4} e^{-i\omega_0 t} e^{-t^2/2} \dots\dots\dots(6)$$

240 where ω_0 is a non-dimensional value. ω_0 is chosen to be 5 to make the highest and lowest
 241 values of ψ approximately equal to 0.5, thus making the admissibility condition satisfied. The
 242 complex valued Morlet transform enables to extract information about the amplitude and
 243 phase of the signal to be analyzed. Wavelet transform preserves the self-similarity scaling
 244 property, which is the inherent characteristic feature of deterministic chaos. The continuous
 245 wavelet transform has edge artifacts because the wavelet is completely localized in time. The
 246 cone of influence (COI) is the area in which the wavelet power caused by a discontinuity at the
 247 edge has dropped to e^{-2} of the value to the edge. The statistical significance of the wavelet

248 power can be assessed relative to the null hypotheses that the signal is generated by a
 249 stationary process with a given background power spectrum (P_k) of first order autoregressive
 250 (AR1) process. (Grinsted et. al., 2004)

251
$$P_k = \frac{1 - \alpha^2}{|1 - \alpha e^{-2i\pi k}|^2} \dots\dots\dots(7)$$

252 where k is Fourier frequency index.

253 The cross wavelet transform is applied to two time series to identify the similar patterns
 254 which are difficult to assess from a continuous wavelet map. Cross wavelet power reveals areas
 255 with high common power. The cross wavelet of two time series x (t) and y (t) is defined as $W^{XY} =$
 256 $W^X W^{Y*}$, where * denotes complex conjugate. The cross wavelet power of two time series with
 257 background power spectra P_k^X and P_k^Y is given as

258
$$D\left(\frac{|W_n^X(s)W_n^{Y*}(s)|}{\sigma_X\sigma_Y} < p\right) = \frac{Z_v(p)}{v} \sqrt{P_k^X P_k^Y}, \dots\dots\dots(8)$$

259 where $Z_v(p)$ is the confidence level associated with the probability p for a pdf defined by the
 260 square root of the product of the two χ^2 distributions (Torrence and Compo, 1998). The
 261 wavelet power is $|W_n^X(s)|^2$ and the complex argument of $|W_n^X(s)|$ can be interpreted as the local
 262 phase. The cross wavelet analysis gives the correlation between the two time series as function
 263 of period of the signal and its time evolution with a 95% confidence level contour. The
 264 statistical significance is estimated using red noise model.

265 Wavelet coherence is another important measure to assess how coherent the cross
 266 wavelet spectrum transform is in time frequency space. The wavelet coherence of two time
 267 series is defined as (Torrence and Webster, 1998)

268
$$R_n^2(s) = \frac{|S(s^{-1}W_n^{XY}(s))|^2}{S(s^{-1}|W_n^X(s)|^2).S(s^{-1}|W_n^Y(s)|^2)} \dots\dots\dots(9)$$

Field Code Changed

Field Code Changed

Field Code Changed

Field Code Changed

$$W_n^2(s) = \frac{|S(s^{-1} W_n^{XY}(s))|^2}{S(s^{-1} |W_n^X(s)|^2) \cdot S(s^{-1} |W_n^Y(s)|^2)} \dots\dots\dots(9)$$

269
 270 where S is a smoothing operator. The smoothing operator is written as $S(W) = S_{scale}(S_{time}(W_n(s)))$, where S_{scale} denotes smoothing along the wavelet scale axis and S_{time} smoothing in
 271 time. Here for the morelet wavelet, the smoothing operator is
 272

$$S_{time}(W)|_s = \left(W_n(s) * c_1 \frac{-t^2}{2s^2} \right) \dots\dots\dots(10)$$

$$S_{time}(W)|_s = (W_n(s) * c_2 \Pi(0.6s))_n | \dots\dots\dots(11)$$

273
 274
 275 Where c_1 and c_2 are normalization constants and n is the rectangle function. The factor of 0.6 is
 276 empirically determined scale decorrelation length of the Morlet wavelet (Torrence and Compo,
 277 1998). The statistical significance level of the wavelet coherence is estimated using the Monte
 278 Carlo methods (Grinsted et. al., 2004).

279
 280 **4. Results and Discussion:**

281 We analyzed the data sets spanning over the period of 1876-2000 using the PCA, SSA and
 282 wavelet spectral analyses. Figure 1 shows four time series: (1) Smoothed Sunspot number
 283 representing solar activities; (2) Geomagnetic (aa indices); (3) Troup Southern Oscillation Index
 284 (SOI) for the study of ENSO and (4) Western Himalayan temperature variability record that are
 285 analyzed in the present work. From visual inspection it is apparent from Fig. 1 that both WH
 286 and SOI data show irregular and random pattern, while sunspot numbers have quasi- cyclic
 287 character. Further WH tree ring record also exhibits distinct temperature variability but
 288 nonstationary behavior at different scales. This variability might be suggestive of coupled
 289 global ocean-atmospheric dynamics or some other factors, such as deforestation,
 290 anthropogenic, high latitudinal influence etc (Yadav et. al., 2004).

291 **(Figure 1)**

292 Hence it is quite difficult to differentiate such a complex climate signals visually and difficult to
293 infer any clear oscillation without the help of powerful mathematical methods. For
294 identification of any oscillatory components and understanding the climatic variations on
295 regional and global scale, we have applied the PCA, SSA and wavelet analysis. Figure 2 shows
296 the principal components (PCs) for the first four eigen triples (PC1, PC2, PC3, PC4) for the given
297 data sets. Figure 3 shows the power spectra of the principal components (PCs) for the four data
298 sets shown in figure 2. From the figure 3, it is observed that the power spectra of PC1-4 for the
299 sunspot data exhibits high power at 124, 11, 4-2.8 years. The presence of high solar signal at
300 124 years indicates the quasi-stable oscillatory components in the data. The power spectra of
301 geomagnetic data also shows the presence of strong signals at 124, 10-11, 4-2 years suggesting
302 a strong link of solar-geomagnetic activity. The power spectra of WH temperature data shows
303 strong high power at ~62 years, 32-35 years, 11 years, 5 years and 2-3 years suggesting a
304 strong influence of solar-geomagnetic-ENSO effects on the Indian climate system. Dominant
305 amplitude is found at 32-35 years corresponding to [Atlantic Multi-decadal Oscillation](#)
306 ~~(AMO)~~ cycles. These results can be better confirmed by applying the mathematical tools of
307 SSA and wavelet analysis.

308 (Figure 2 & 3)

309 To explore the stationary characteristics of these peaks obtained by the PCA, we have applied
310 the Morlet based wavelet transform approach (Holschneider, 1995; Foufoula-Georgiou and
311 Kumar, 1995; Torrence and Compo, 1998; Grinsted et. al., 2004). The wavelet spectrum
312 identifies the main periodicities in the time series and helps to analyze the periodicities with
313 respect to time. Figure 4 shows the wavelet spectrum for the a) Smoothed Sunspot number for
314 solar activity (SSN) (b) Western Himalayan (WH) temperature variability record (c) Geomagnetic
315 activity and (c) Troup Southern Oscillation Index (SOI). From the wavelet spectrum of sunspot
316 time series (Figure 4a), the signal near 11-year is the strongest feature and is persistent during
317 the entire series indicating the non-stationary behavior of the sunspot time series. The wavelet
318 spectrum of SOI (figure 4c) shows strong amplitudes. However, due to non-stationary (time
319 variant) character of the time series, the observed spectral peaks (power) split—but
320 nonstationary in the interval of 2- 8 years. The wavelet power spectrum of the western

321 Himalayan temperature variability (Figure 4b) reveals significant power concentration at inter-
322 annual time scales of 3-5 years and at 11 years solar cycle. A dominant amplitude modes is also
323 seen in the low frequency range at around 35-40 years (at periods 1930-1980) corresponding to
324 AMO cycles. Our result agrees well with the results of other climate reconstructions (Mann et.
325 al., 1995) from tree rings and other proxies. The observed variability in AMO periodicity has also
326 been reported in other tree ring record (Gray et. al., 2004). The statistical significance of the
327 wavelet power spectrum is tested by a Monte Carlo method (Torrence and Compo, 1998). The
328 WH spectra depicting statistically significant powers at around 5 years, 11 years and 33 years
329 above the 95% significance level, suggests a clear picture of the imprint of sunspot-geomagnetic
330 and ENSO on the tree ring data. The wavelet power spectrum of the geomagnetic record (Fig.
331 4d) indicates significant power on shorter scales around 2, 4-8, 11 years period.

332 **(Figure 4)**

333 In order to have better visualization of similar periods in two time series and for the
334 interpretation of the results, cross wavelet spectrum has been applied. Figure 5 shows the cross
335 wavelet spectrum of the a) SSN-WH temperature data b) WH data-SOI and c) SSN-SOI data. The
336 contours (dark black lines) are the enclosing regions where wavelet cross power is significantly
337 higher, at 95% confidence levels. The wavelet cross-spectra of WH-SSN (Fig.5a) show
338 statistically significant high power over a period of 1895-1985 in 8-16 years band. It is seen that
339 the WH-SOI cross-spectra (Fig. 5b), the high power is observed at 2-4 year band and 8-16 years
340 as well. The SSN-SOI spectra (Fig. 5c) shows a strong correlation at 11 years solar cycle, which is
341 stronger during 1910-1950 and 1960-2000 (Rigozo et. al., 2002, Rigozo et. al., 2003) suggesting
342 the strongest El Nino and La Nina events indicating solar modulation on ENSO ([Kodera, 2005;](#)
343 [Kryjov and Park, 2007](#)):- These results show a good correspondence in response of growth of
344 the tree ring time series during the intense solar activity. Hence the results strongly support the
345 possible origin of these periodicities from Solar and ENSO events. The interesting conclusion
346 from Fig. 5 is that WH-sunspot connections are strong at 11 years, ENSO-sunspot also exhibit
347 strong power around 11 years; the WH-ENSO connections are spread over three bands, the 2-4
348 y; 4-8 and 8-16 y, covering the solar cycle and its harmonics; the WH-geomagnetic exhibits

349 strong connections around 2-4, 4-6, 11 years and 35-40 years indicating the influence of solar-
350 geomagnetic activity on Indian temperature.

351 **(Figure 5)**

352

353 The Singular spectral analysis (SSA) is performed for all the four data sets with window length of
354 40. The SSA spectra with 40 singular values and its corresponding reconstructed series (varying
355 from RC1-15 in some cases) are plotted are shown in Figure 6 & 7. The important insights from
356 SSA spectra are the identification of gaps in the eigen value spectra. As a rule, the pure noise
357 series produces a ~~slowly~~ decreasing sequence of singular values. The explicit plateau in
358 the spectra represents the ordinal numbers of paired eigen triples. The eigen triples 2-3 for the
359 sunspot data corresponds to 11 years period; eigen triples for 1-2,3-5,6-10,11-14 for the WH
360 temperature data are related to harmonic with specific periods (periods 33-35, 11, 5, 2); eigen
361 triples for 2-5,6-9,10-13 for the geomagnetic data are related to periods 11, 5, 2 years. The
362 eigen triples for the SOI data represents to ~ 5-7, 2 years periods. In order to assess
363 periodicities, the periodogram and the wavelet power spectra are plotted using the SSA
364 reconstructed data (SSA-RC) (Figure 8). From the figure 8, the periodogram of SSA-RC of SSN
365 and Geomagnetic data shows strong power at ~120, 10-11 years; the SOI data shows strong
366 peaks at 6-9, 3, years & WH data shows strong power at ~32, ~10-11, 3-5 years. The wavelet
367 spectra for all the SSA-RC data confirms the results excepts for periods at ~120 years as the
368 scaling period for the wavelet spectra is 64 years period. The coherency plot of the SSA-RC data
369 sets (Figure 9) indicates a significant power at 33 years, 11 years, 2-7 years in the WH
370 temperature record suggesting the possible influences of Sunspot-geomagnetic activity and
371 ENSO through tele-connection and hence significant role of these remote internal oscillations of
372 the atmosphere-ocean system on the Indian climate system. Researchers have attributed these
373 phenomena to internal ocean dynamics and involve ocean atmospheric coupling as well as
374 variability in the strength of thermohaline circulations (Knight et. al., 2005; Delworth and Mann,
375 2000).

376

(Figures 6, 7, 8 & 9)

377 | In general our result agrees well with earlier findings in [the](#) sense that statistically
378 significant global cycles of coupled effects of Sunspot/geomagnetic and ENSO are present in the
379 land based temperature variability record. However, there are certain striking features in the
380 spectra that need to be emphasized regarding the western Himalayas temperature variability: i)
381 Inter-annual cycles in period range of 3-8 years corresponding to ENSO in the wavelet spectra
382 exhibit intermittent oscillatory characteristics throughout the large portion of the record (Fig 4);
383 ii) The 11 years solar cycle in the cross wavelet spectrum of SSN and SOI (Figure 5) indicate the
384 solar modulation in the ENSO phenomena ([Kodera, 2005; Kryjov and Park, 2007](#));- iii) The high
385 amplitude at 11 years in the time intervals 1900-1995 with a strong intensity from 1900-1995
386 shows a good correspondence with the high temperature variability for the interval of high
387 solar-geomagnetic activity. The Multi-decadal (30-40 years) periodicity identified here in
388 Western Himalayan tree ring temperature record matches with North Atlantic sea surface
389 temperature variability implying that the temperature variability in the western Himalayan is
390 not a regional phenomenon, but a globally tele-connected climate phenomena associated with
391 the global ocean-atmospheric dynamics system (Tiwari & srilakshmi, 2009; Delworth et. al.,
392 1993; Stocker, 1994). The coupled ocean-atmosphere system appears to transport energy from
393 the hot equatorial regions towards Himalayan territory in a cyclic manner. These results may
394 provide constraints for modeling of climatic variability over the Indian region and ENSO
395 phenomena associated with the redistribution of temperature variability. The solar-
396 geomagnetic effects play a major role in abnormal heating of the land surface thereby indirectly
397 affects the atmospheric temperature gradient between the land-ocean coupled systems. In the
398 present work, the connections between solar/geomagnetic activity and ENSO on the WH time
399 series are found to be statistically significant, especially when they are studied over contrasting
400 epochs of respectively high and low solar activity. The correlation plots for the SSA-RC data sets
401 of WH-sunspot, WH-aa index, WH-SOI and Sunspot-aa index are plotted in figure 10. It is
402 noticed that there is a correlation plots for the Geomagnetic-sunspot activity has a maximum
403 correlation value at 1 year lag suggesting the strong influence of sunspot & geomagnetic forcing
404 on one another. The cross-correlation plot for the WH data and the SOI represents a maximum
405 value at zero lag. The correlations plot for WH-sunspot & WH-geomagnetic index exhibits

406 almost the identical results suggesting the possible impact of solar activities on the Indian
407 temperature variability.

408 **(Figures 10)**

409 The net effect of solar activity on temperature record therefore appears to be the result
410 of cooperating or counteracting influences of earth's magnetic activity on the shorter and
411 longer periods, depending on the indices used; scale-interactions, therefore, appear to be
412 important. Nevertheless, the link between Indian climate and solar/geomagnetic activity
413 emerges as having the strong evidence; next is the ENSO-solar activity connection.

414

415 **5. Conclusions:**

416 In the present paper, we have studied ~~and~~ identified the periodic patterns from the published
417 Indian temperature variability records using the modern spectral methods. ~~This study of~~
418 Singular spectral analysis (SSA)-Wavelet ~~spectral~~ methods. ~~The on the data sets and the~~
419 application of wavelet analysis for the SSA reconstructed time series, ~~along with highlights~~ the
420 removal of noise in the data ~~and~~ identifies the existence of a high-amplitude, recurrent, multi-
421 decadal scale patterns that are present in Indian temperature records. ~~The power~~
422 ~~spectra~~ ~~Wavelet spectral analysis~~ of ~~WH temperature SSA reconstructed~~ data ~~shows strong high~~
423 ~~power at ~62 years, 32-35~~ identifies significant peaks around ~~33~~ years, 11 years, 5 years and 2-3
424 ~~years suggesting a strong influence of solar-geomagnetic-ENSO effects on 2-7 years (95%~~
425 ~~confidence) in the Indian climate system. Western Himalayan (WH) temperature record. The~~
426 presence of ~~dominant amplitude at 33~~ year cycle periodicity ~~corresponds to Atlantic~~
427 ~~Multidecadal Oscillation (AMO) cycles. It also~~ suggests the Sun-temperature variability probably
428 involving the induced changes in the basic state of the atmosphere. The 30-40 yrs periodicity in
429 Western Himalayan tree ring temperature record matches with the global signal of the coupled
430 ocean-atmospheric oscillation (Delworth et. al., 1993; Stocker, 1994) implying that the
431 temperature variability in Himalayan is not a regional phenomenon, but seems to be tele-
432 connected phenomena with the global ocean-atmospheric climate system. The coherency plots
433 of the SSA reconstructed WH-Sunspot; WH-geomagnetic and WH-SOI data sets show strong
434 spectral signatures in the whole record confirming the possible influences of Sunspot-

Formatted: Font color: Auto

Formatted: Font color: Auto

Formatted: Font color: Auto

Formatted: Font color: Auto

435 geomagnetic activities and ENSO through teleconnection and hence the significant role of
436 these remote internal oscillations of the atmosphere-ocean system on the Indian temperatures.
437 We conclude that the signature of solar-geomagnetic activity affects the surface air
438 temperatures of Indian subcontinent. However, long data sets from the different sites on the
439 Indian continent are necessary to identify the influences of the 120 years solar-geomagnetic
440 cycles.

441

442 Acknowledgements

443 The authors are extremely thankful to the anonymous reviewers for their professional
444 comments, meticulous reading of the manuscript and valuable suggestions to improve the
445 manuscript. The authors thank Dr. ~~Ram Ratan R. Yadav~~, Birbal Sahni Institute of
446 Palaeobotany, India for providing the Western Himalayan data. The authors acknowledge Dr.
447 Francisco Javier Alonso of University of Extremadura for using the SSA routine in a MATLAB
448 environment. ~~his data~~. We are thankful to Dr. Grinsted and his colleagues for providing
449 the wavelet software package. ~~First author acknowledged we are very grateful to~~
450 the Head, University Centre for Earth & Space Sciences, UCESS, University of Hyderabad for
451 providing the facilities to carry out ~~his support and kind permission to~~
452 publish this work. RKT is grateful to DAE for RRF. ~~paper.~~

453

454 References

455 Alonso, F. J., Castillo, J., and Pintado, P. (2005), "Application of Singular Spectrum Analysis to the
456 Smoothing of Raw Kinematic Signals," Journal of Biomechanics, 38(5), 1085–1092.
457 Appenzeller, C., Stocker, T. F., and Anklin, M. (1998). North Atlantic Oscillation Dynamics Record in
458 Greenland Ice Cores. *Science*, 282(5388), 446–449.
459 Barnett, T.P., et al. (1989). The effect of Eurasian snow cover on regional and global climate
460 variations. *J. Atmos. Sci.*, 48, 661–685.
461 Benestaed, R.E., and Schmidt, G.A., (2009), Solar trends and global warming, *Journal of Geophysical*
462 *research*, P 114.

Formatted: Font: + Body

Formatted: HTML Preformatted

Formatted: Font: + Body

Formatted: Font: + Body

Formatted: Font: + Body

Formatted: Font: + Body, Font color: Auto

Formatted: Font: + Body

Formatted: Font: + Body

Formatted: Font: + Body

Formatted: Font: + Body

Formatted: Font: + Body, English (India)

463 Bhattacharyya A, LaMarche VC, and Telewski FW, (1988) Dendrochronological reconnaissance of the
464 conifers of Northwest India, *Tree-Ring Bull.*, 48: 21-30.

465 Bhattacharyya A, and Chaudhary V, (2003) Late-summer temperature reconstruction of the Eastern
466 Himalayan Region based on tree-ring data of *Abies densa*, *Arct. Antarct. Alp.Res.*, 35(2): 196-202.

467 Bhattacharyya A, and Yadav RR, (1996) Dendrochronological reconnaissance of *Pinus wallichiana* to
468 study glacial behaviour in the western Himalaya. *Current Science*, 70 (8): 739-744.

469 Bhattacharyya A, Shah, Santosh K, and Chaudhary V, (2006) Would tree-ring data of *Betula utilis* be
470 potential for the analysis of Himalayan Glacial fluctuations?, *Current Science*, 91(6): 754-761.

471 Bhattacharyya A, Yadav RR, Borgaonkar HP, & Pant GB, (1992) Growth ring analysis of Indian tropical
472 trees: Dendroclimatic potential, *Current Science*, 62: 736-741.

473 Bhattacharyya, A. and Yadav, R.R., (1992) Tree growth and recent climatic changes in the western
474 Himalaya, *GeophytoJogy*, 22, 255-260.

475 Bigg GR, (1996) *The oceans and Climate*, Cambridge University Press, Cambridge, 1-266.

476 Borgaonkar HP, Pant GB, & Rupa Kumar k, (1996) Ring width variations in *Cedrus deodara* and its
477 climatic response over the Western Himalaya. *Intern. J. Climatol.* 16: 1409-1422.

478 Broomhead, D.S., and King, G.P., (1986). Extracting qualitative dynamics from experimental data,
479 *Physica D* 20, 217–236.

480 Budyko, M. I. (1969). The effect of solar radiation variations on the climate of the Earth. *Tellus*, 21,
481 611–619

482 Cane MA, (1992) Tropical Pacific ENSO models: ENSO as a mode of the coupled system. In: *Climate*
483 *System Modelling*, Ed: K.E. Trenberth, Cambridge University Press, Cambridge, 583-614.

484 Chaudhary V, Bhattacharyya A, and Yadav RR, (1999) Tree-ring studies in the Eastern Himalayan
485 region: Prospects and problems, *IAWA*, .20(3): 317-324.

486 Chowdary, J. S., John, N., and Gnanseelan, C. (2014). Interannual variability of surface air-
487 temperature over India: impact of ENSO and Indian Ocean Sea surface temperature. *Int. J.*
488 *Climatol.*, 34, 416–429.

489 Chowdary, J.S., Gnanseelan, C., Vaid, B.H., and Salvekar, P.S. (2006). Changing trends in the tropical
490 Indian Ocean SST during La Nina years. *Geophys. Res. Lett.*, 33, L18610. doi:10.1029/
491 2006GL026707.

492 Cole JE, Fairbanks RG, and Shen GT, (1993) Recent variability in the Southern Oscillation: Isotopic
493 results from a Tarawa Atoll coral. *Science*, 260: 1790-1793.

494 De Freitas, C., and Mclean, J. (2013). Update of the Chronology of Natural Signals in the Near-Surface
495 Mean Global Temperature Record and the Southern Oscillation Index. *International Journal of*
496 *Geosciences*, 4 (1), 234–239.

497 Delworth T, and Mann M, (2000) Observed and Stimulated multidecadal variability in the Northern
498 Hemisphere, 16: 661-676.

499 Delworth T, Manabe S & Stouffer RJ (1993) Interdecadal variations of the thermohaline circulation in
500 a coupled ocean-atmosphere model. *J. Climate* 6: 1991-2011.

501 El-Borie, M.A., Shafik, E., Abdel-Halim, A.A., El-Monier, S., (2010), Spectral analysis of solar
502 variability and their possible role on the global warming (1880-2008), *Journal of Environmental*
503 *Protection*, 1, pp 111-120.

504 El-Borie, M.A., Al. Thoyaib, S.S, Al-Sayed, N., (2007), *The 2nd Inter. CPMS*, 302.

505 El-Borie, M.A., and Al-Thoyaib, S.S., (2006), Can we use the aa geomagnetic activity index to predict
506 partially the variability in global mean temperature, *Journal of Physical Sci.*,1(2), pp 67–74.

507 Feng, S.H., Kaufman, D., Yoneji, S., Nelson, D., Shemesh, A., Huang, Y., Tian, J., Bond, G., Benjamin, C.,
508 and Brown, T. (2003). Cyclic Variation and Solar Forcing of Holocene Climate in the Alaskan
509 Subarctic. *Science*, 301, 1890–1893.

510 Foufoula-Georgiou E, and Kumar P, (Eds.), (1995) *Wavelets in Geophysics*, Academic San Diego, Calif.,
511 373pp.

512 Friis, C.E., and Lassen, K. (1991). Length of the Solar Cycle: An Indicator of Solar Activity Closely
513 Associated with Climate. *Science*, 254 (5032), 698–700.

514 Friis, C.E., and Svensmark, H. (1997). What do we really know about the sun- climate connection?,
515 *Adv. Space Res.*, 20, 415, 913–9211.

516 Frohlich, C., and Lean, J. (2004). Solar radiative output and its Variability: Evidence and Mechanisms.
517 *The Astron Astropys Rev.*, 12, 273–320.

518 [Golyandina, N., Nekrutkin, V. V., and Zhigljavski, A. A. \(2001\), Analysis of Time Series Structure:](#)
519 [SSA and Related Techniques, Boca Raton: CRC Press.](#)

520 Gray L.J., Beer, J., Geller, M., Haigh, J.D., Lockwood, M., Matthes, K., Cubasch, U., Fleitmann, D.,
521 Harrison, G., Hood, L., Luterbacher, J., Meehl, G.A., Shindell, D., van Geel, B., and White, W., (2010).
522 Solar influences on climate, *Reviews of Geophysics*, 48, RG 4001, doi: 10.1029/2009RG000282.

523 Gray ST, Graumlich LJ, Betancourt JL, and Pederson GT, (2004) A tree-ring based reconstruction of the
524 Atlantic Multidecadal Oscillation since 1567 A.D, *Geophys. Res. Lett.*, 31: L12205,
525 doi:10.1029/2004GL019932.

526 Gray, W. M., Sheaffer, J. D., and Knaff, J. A. (1992). Hypothesized mechanism for stratospheric QBO
527 influence on ENSO variability. *Geophys. Res. Lett.*, 19, 107–110.

528 Grinsted A, Moore JC, Jevrejeva S (2004) Application of the cross wavelet transform and wavelet
529 coherence to geophysical time series, *Nonlin. Processes Geophys.*, 11: 561–566,
530 doi:10.5194/npg-11-561-2004

531 Gu, D., and Philander, S.G.H., (1995). Secular changes of annual and inter-annual variability in the
532 tropics during the past century, *J. Clim.* 8, 64–876.

533 Holschneider M (1995) *Wavelets: An Analysis Tool*, Oxford University Press, New York, 455.

534 Horel, J.D., and Wallace, J.M. (1981). Planetary-scale atmospheric Phenomena associated with the
535 Southern Oscillation, *Monthly weather review*, 109, 813-829.

536 Hughes MK (1992) Dendroclimatic evidence from the Western Himalaya. In: R.S. Bradley &
537 D. Jones (eds.), *Climates since AD 1500*: 4 15-431. Routledge, London.

538 Jevrejeva S, Moore JC, Grinsted A (2003) Influence of the Arctic Oscillation and El Niño-Southern
539 Oscillation (ENSO) on ice conditions in the Baltic Sea: The wavelet approach, *J. Geophys. Res.*,
540 108(D21), 4677, doi:10.1029/2003JD003417.

541 Ji JF, Shen J, Balsam W, Chen J, Liu L & Liu XQ, (2005) Asian monsoon oscillations in the northeastern
542 Qinghai-Tibet Plateau since the late glacial as interpreted from visible reflectance of Qinghai Lake
543 sediments, *Earth and Planetary Science letters* 233: 61-70.

544 Kasatkina, E.A., Shumilov, O.I., and Krapiec, M. (2007). On periodicities in long term climatic variations
545 near 68_N, 30_E. *Adv. Geosci*, 13, 25–29.

546 Kiladis, G.N., and Diaz, F.H. (1989). Global Climatic Anomalies Associated with Extremes in the
547 Southern Oscillation. *J. Climate*, 2, 1069–1090.

548 Knight JR, Allan RJ, Folland CK, Vellinga M, and Mann ME, (2005) A signature of persistent natural
549 thermohaline circulation cycles in observed climate'. *Geophys. Res. Lett.*, 32, L20708,
550 doi:10.1029/2005GL024233.

551 ~~[Kodera, K., and Y.Kuroda \(2005\). A possible mechanism of the spatial structure of the North Atlantic](#)~~
552 ~~[Oscillation, *Journal of Geophysics Research*, 110, D02111, doi: 10.1029/2004JD005258.](#)~~

553 Kothwale, D.R., Munot, A.A., and Krishna Kumar, K. (2010). Surface air temperature variability over
554 India during 1901-2007 and its association with ENSO. *Climate Research*, 42, 89–104,
555 doi:10.3354/cr00857.

556 ~~[Kryjov, V.N., and Park, Chung-Kyu, \(2007\). Solar modulation of the El-Nino/Southern Oscillation](#)~~
557 ~~[impact on the Northern Hemisphere annular mode, *Geophysical research letters*, Vol. 34,](#)~~
558 ~~[L10701, doi: 10.1029/2006GL028015.](#)~~

559 ~~[Labitzke K and Van Loon H, \(1989\) Association between the 11-Year Cycle, the QBO and the](#)~~
560 ~~[Atmosphere, *Journal of Climate*, 2.](#)~~

561 ~~[Labitzke K and Van Loon H, \(1992\) Association between the 11-Year solar cycle and the Atmosphere.](#)~~
562 ~~[Part V: Summer, *J. Climate*, 5: 240-251.](#)~~

563 ~~[Labitzke K and Van Loon H, \(1993\) Some recent studies of probable connections between solar and](#)~~
564 ~~[atmospheric variability, *Ann. Geophysicae*, 11.](#)~~

565 ~~[Lean and Rind, 2008](#)~~; Lean, J.L. and Rind, D.H., (2008), How natural and anthropogenic influences
566 alter global and regional surface temperatures: 1889 to 2006, *Journal of Geophysical*
567 *Research, Letter*, p 35.

568 Lean, J., Beer, J., and Bradley, R. (1995). Reconstruction of solar irradiance since 1610: Implications
569 for climate change. *Geophys. Res.Lett.*, 22, 3195-3198.

570 Mann ME, Park J, and Bradley RS, (1995) Global interdecadal and century-scale climate oscillations
571 during the past 5 centuries, *Nature*, 378: 266–27.

572 Meehl, G.A., Arblaster, J.M., Matthes, K., Sassi, F., and Van Loon, H. (2009). Amplifying the Pacific
573 climate system response to a small 11-year solar cycle forcing. *Science*, 325, 1114–1118.

574 Mendoza B, Perez-Enriquez R, and Alvarez-Madrigal M, (1991) Analysis of solar activity conditions
575 during periods of El Nino events, *Ann. Geophysicae*, 9: 50-54.

576 Mokhov, I. I., Eliseev, A.V., Handorf, D., Petukhov, V.K., Dethloff, K., Weishiemer, A., and
577 Khvorostyanov, D. V. (2000). North Atlantic Oscillation: Diagnosis and simulation of decadal
578 variability and its long period evolution. *Atmospheric and Ocean physics*, 36, 555–565.

579 Nicolson, S. E. (1997). An analysis of the Enso signal in the tropical Atlantic and western Indian
580 oceans. *Int. J. Climatol.*, 17, 345–375.

581 Pant, G.B., and Rupa Kumar, K. (1997). *Climates of South Asia*. John Wiley and Sons, Chichester, 320
582 pp.

583 Philander SG, (1990) El Nino, La Nina and the Southern Oscillation. Academic Press, London, 1-293.

584 Proctor, C.J., Baker, A., and Barnes, W. L. (2002). A three thousand year record of North Atlantic
585 Climate. *Clim.Dyn*, 19, 449–454.

586 Reid GC and Gage KS, (1988) The climatic impact of secular variations in solar irradiance, in *Secular*
587 *Solar and geomagnetic Variations in the Last 10000 years'*, Eds. F.R. and A.W. Wplfendale, NATO
588 AS Series, Kluwer, Dordrecht, 225-243.

589 Reid GC, (1991) Solar irradiance variations and global Ocean Temperature, *Journal of Geomagn.*
590 *Geoelectr.*, 43: 795-801.

591 Rigozo NR, Noredmann DJR, Echer E, Zanandrea A, Gonzalez WD, (2002) Solar variability effects
592 studied by tree-ring data wavelet analysis, *Adv. Space Res.*, 29(12): 1985-1988.

593 Rigozo NR, Vieira Lea, Echer E, Nordemann DJR, (2003) Wavelet analysis of Solar-ENSO imprints in
594 tree-ring data from Southern Brazil in the last century, *Climatic change*, 60: 329-340.

595 Rigozo, N. R., Nordeman, D. J. R., Echer, E., Vieira, L. E. A., Echer M. P. S. and Presets, A.(2005). Tree-
596 ring width wavelet and spectral analysis of solar variability and climatic effects on a Chilean
597 cypress during the last two and a half millennia. *Climate of the Past Discussions*, 1, 121–135.

598 Rigozo, N. R., Nordeman, D.J.R., Silva, H.E., Echer, M.P.S. and Echer, E. (2007). Solar and climate signal
599 records in tree ring width from Chile (AD1587–1994). *Planetary and Space Science*, 55, 158–164.

600 Shah Santosh K, Bhattacharyya A, and Chaudhary V, (2007) Reconstruction of June-September
601 Precipitation based on tree-ring data of Teak (*Tectona grandis* L.) from Hoshangabad, Madhya
602 Pradesh, India. *Dendrochronologia*, 25: 57-64.

603 Steinhilber, F., Beer, J. and Frohlich, C. (2009). Total solar irradiance during the Holocene. *Geophys.*
604 *Res. Lett.*, 36, L19704.

605 Stocker TF (1994). The variable ocean. *Nature* 367: 221-222.

606 Tiwari RK, and Srilakshmi S, (2009). Periodicities and non-stationary modes in tree ring temperature
607 variability record of the Western Himalayas by multitaper and wavelet spectral analyses, *Current*
608 *Science*, 97, 5: 705-709.

609 Torrence C, Compo GP, (1998). A practical guide to wavelet analysis, *Bull. Am. Meteorol. Soc.*, 79: 61–
610 78

611 Torrence C, Webster P, (1999). Interdecadal changes in the ENSO-Monsoon System, *J.Clim.*, 12:
612 2679–2690.

613 Trenberth K, and Hoar TJ, (1997). El Nino and climate change. *Geophys. Res. Lett.*, 24: 3057–3060.

614 Tsonis, A. A., Elsner, J. B., Hunt, A. G., and Jagger, T. H. (2005). Unfolding the relation between global
615 temperature and ENSO. *Geophys.Res.Lett.*, 32, L09701.

616 Vautard, R., and Ghil, M. (1989). Singular spectrum analysis in nonlinear dynamics, with applications
617 to paleoclimatic time series. *Phys. D*, 35, 395–424.

618 Weng, H., and K.-M. Lau, 1994: Wavelets, period doubling, and time-frequency localization with
619 application to organization of convection over the tropical western Pacific. *J. Atmos. Sci.*, 51,
620 2523–2541.

621 Wiles, G. C., D'Arrigo, R. D., and Jacoby, G. C. (1998). Gulf of Alaska atmosphere-ocean variability over
622 recent centuries inferred from coastal tree-ring records, *Climatic Change*, 38,

623 Yadav RR, Park WK, and Bhattacharyya A, (1999) Spring-temperature variations in western Himalaya,
624 India, as reconstructed from tree-rings: AD 1390-1987, *The Holocene*, 9(1): 85-90.

625 Yadav RR, Park WK, Singh J & Dubey B, (2004) Do the western Himalayas defy global warming?.,
626 *Geophysical Research Letters* 31: L17201, doi: 10.1029/2004GL020201.

627 Yasunari, T. (1985). Zonally propagating modes of the global east–west circulation associated with
628 the Southern Oscillation. *J. Meteorol. Soc. J.*, 63, 1013–1029.

629

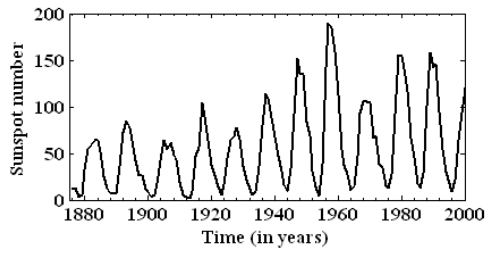
630

631

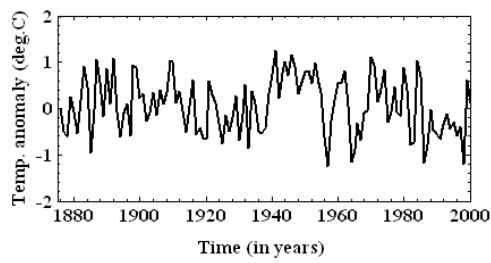
632

633

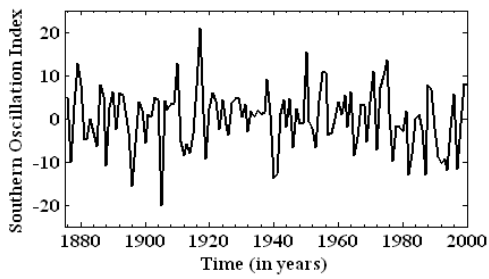
634
635
636
637
638
639
640
641



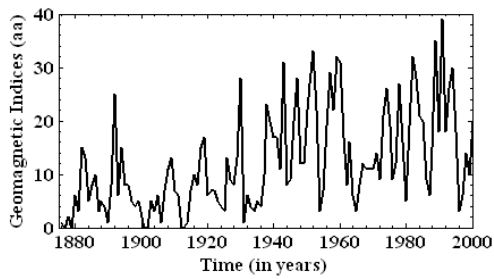
(a)



(b)



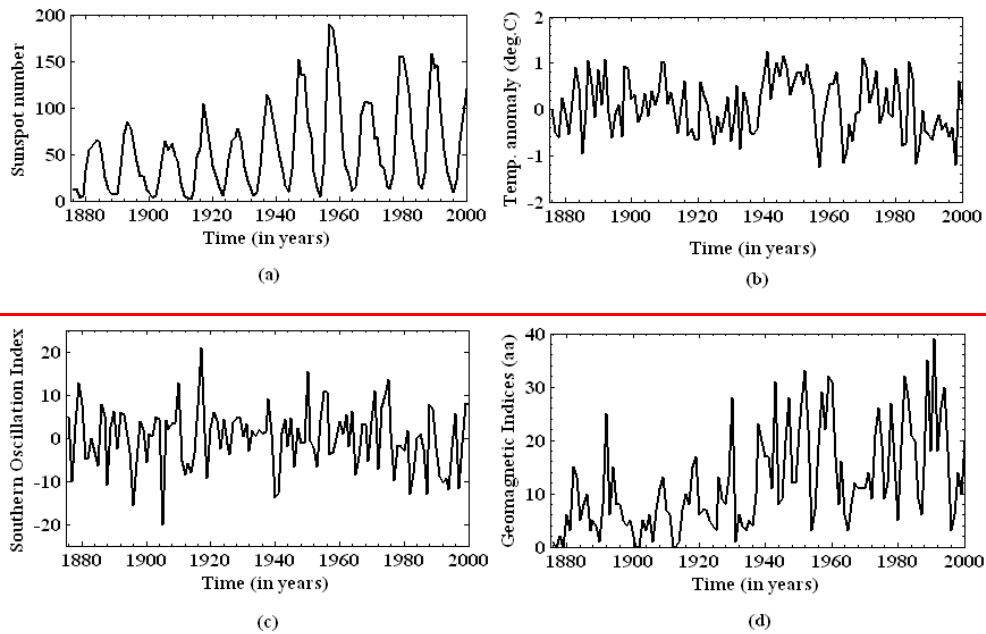
(c)



(d)

642

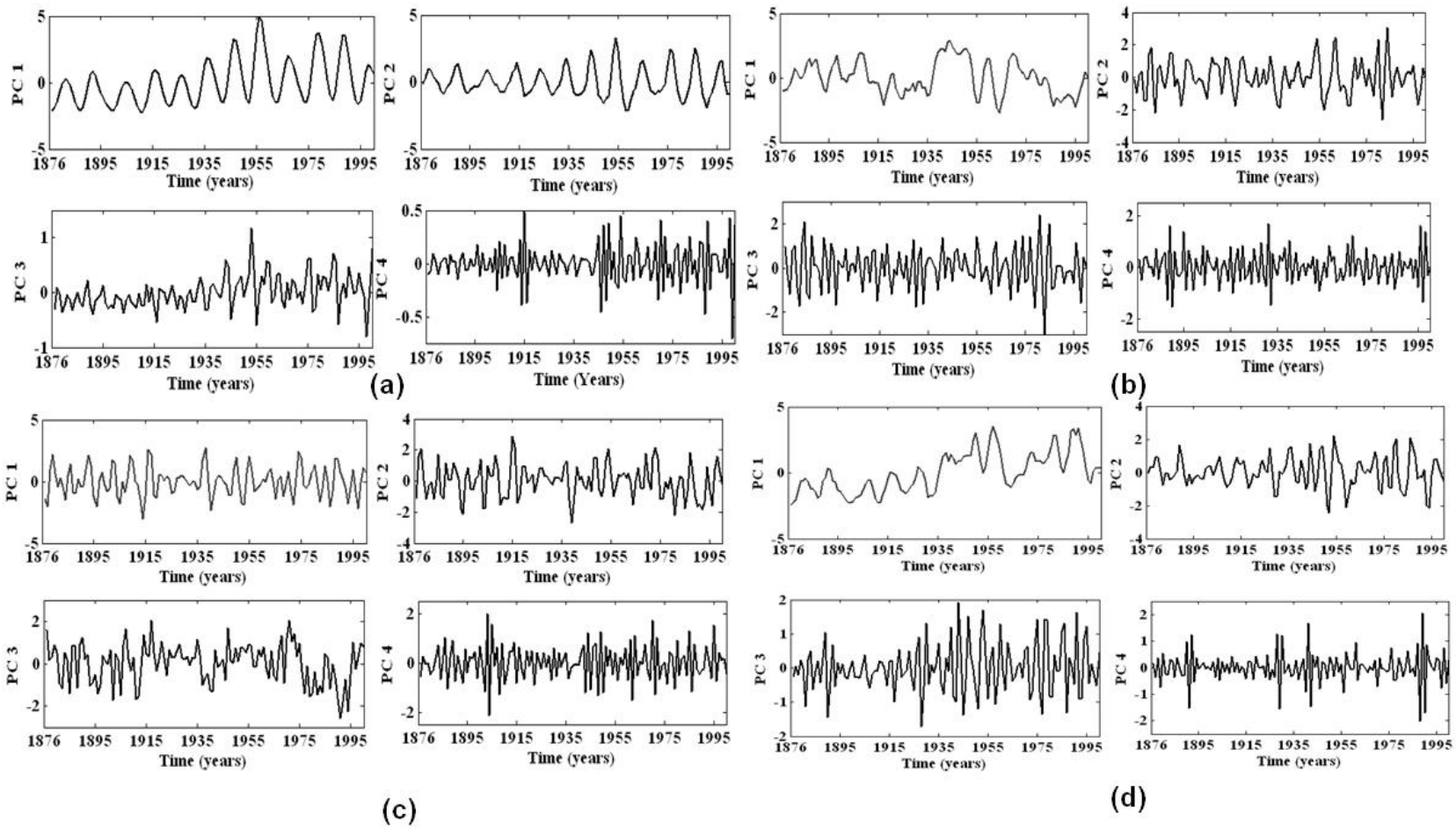
Formatted: Font: 12 pt, Bold



643
 644 **Figure 1. Time series data of (a) Sunspot Index (b) the mean pre-monsoon temperature**
 645 **anomalies of the Western Himalayas ([Yadav et. al., 2004](#)) (c) Southern Oscillation Index**
 646 **(SOI) and (d) Geomagnetic Indices (aa indices) for common period 1876-2000.**

647

648



649
650

Figure

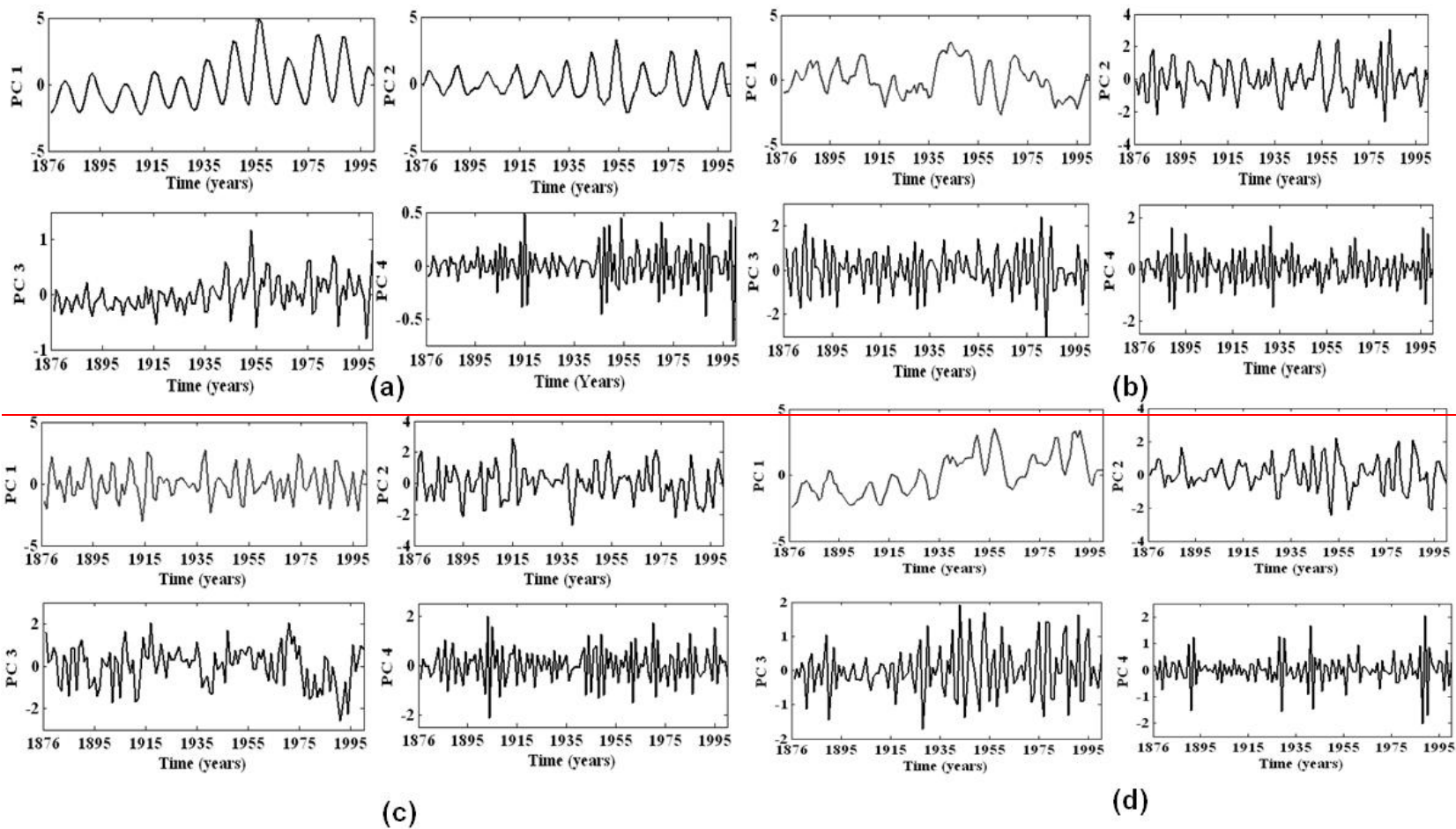
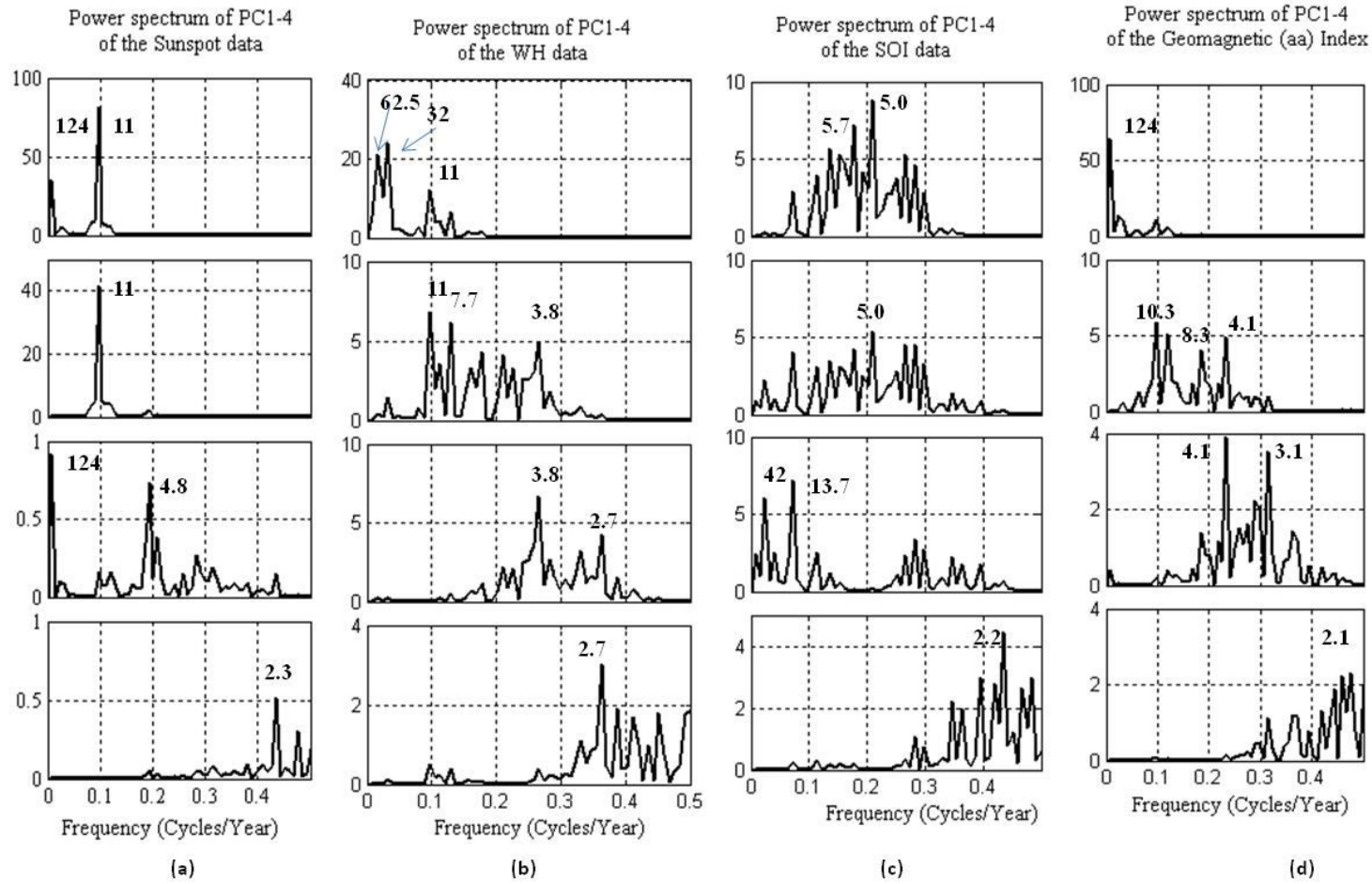
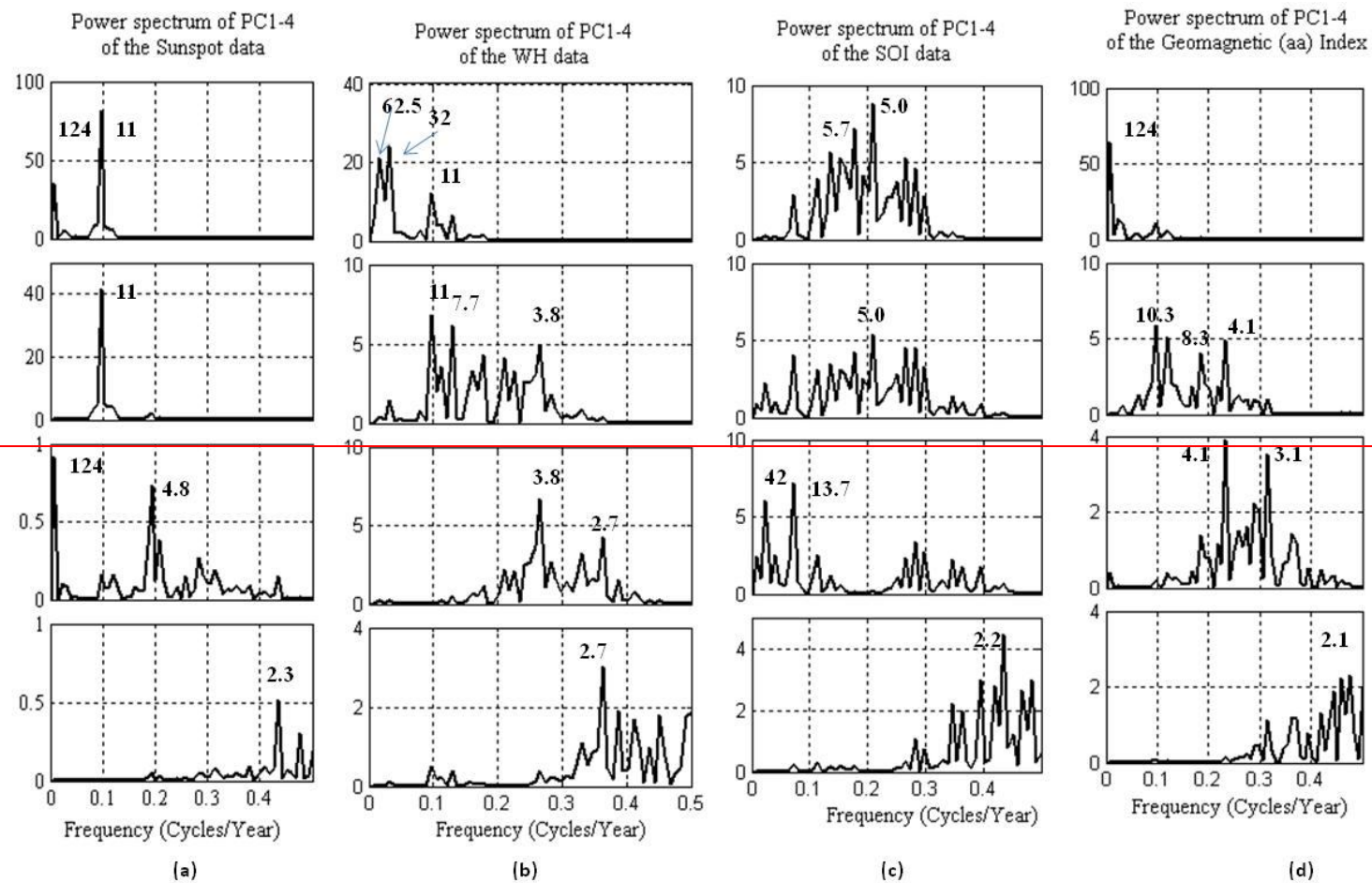


Figure 2. First four principal components (PCs:1-4) for time series (a) Sunspot numbers (b) the mean pre-monsoon temperature anomalies of the Western Himalayas (c) SOI index and (d) Geomagnetic Indices (aa indices) for the period 1876-2000.

Formatted: Font: 12 pt

651
652
653





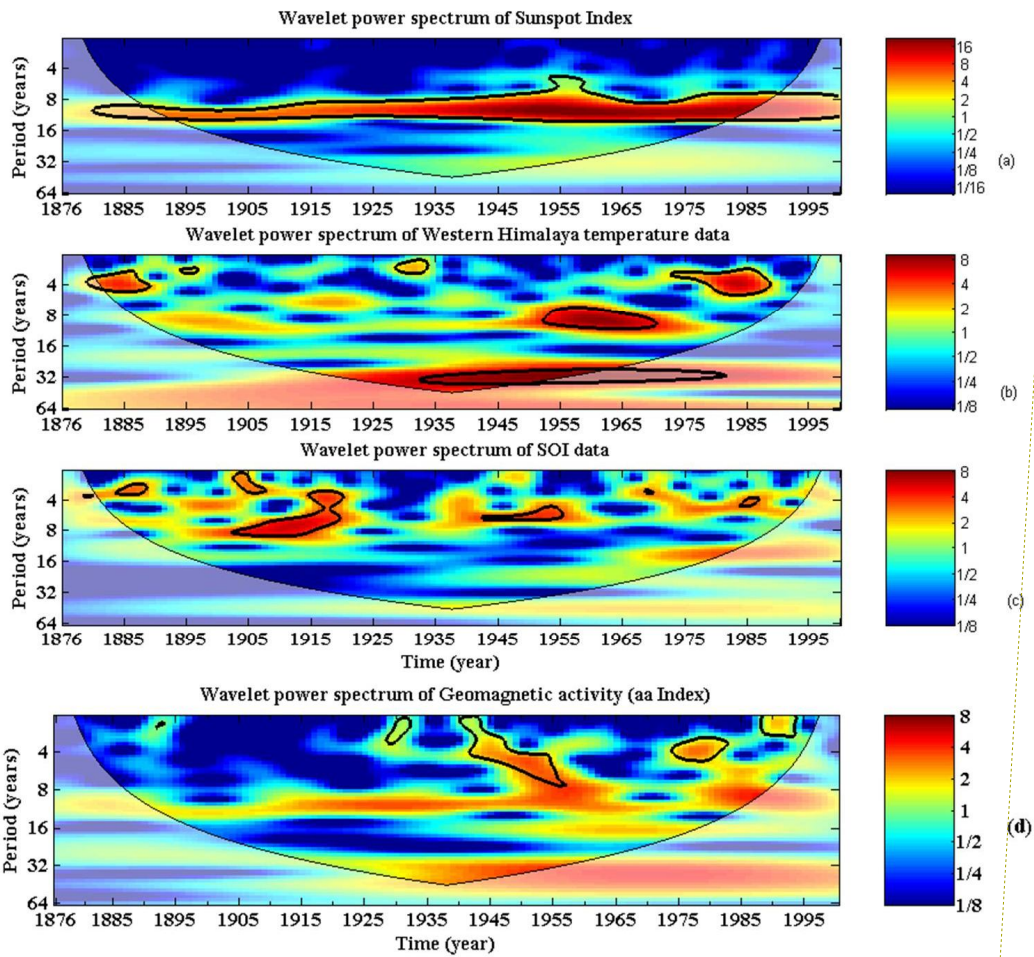
655

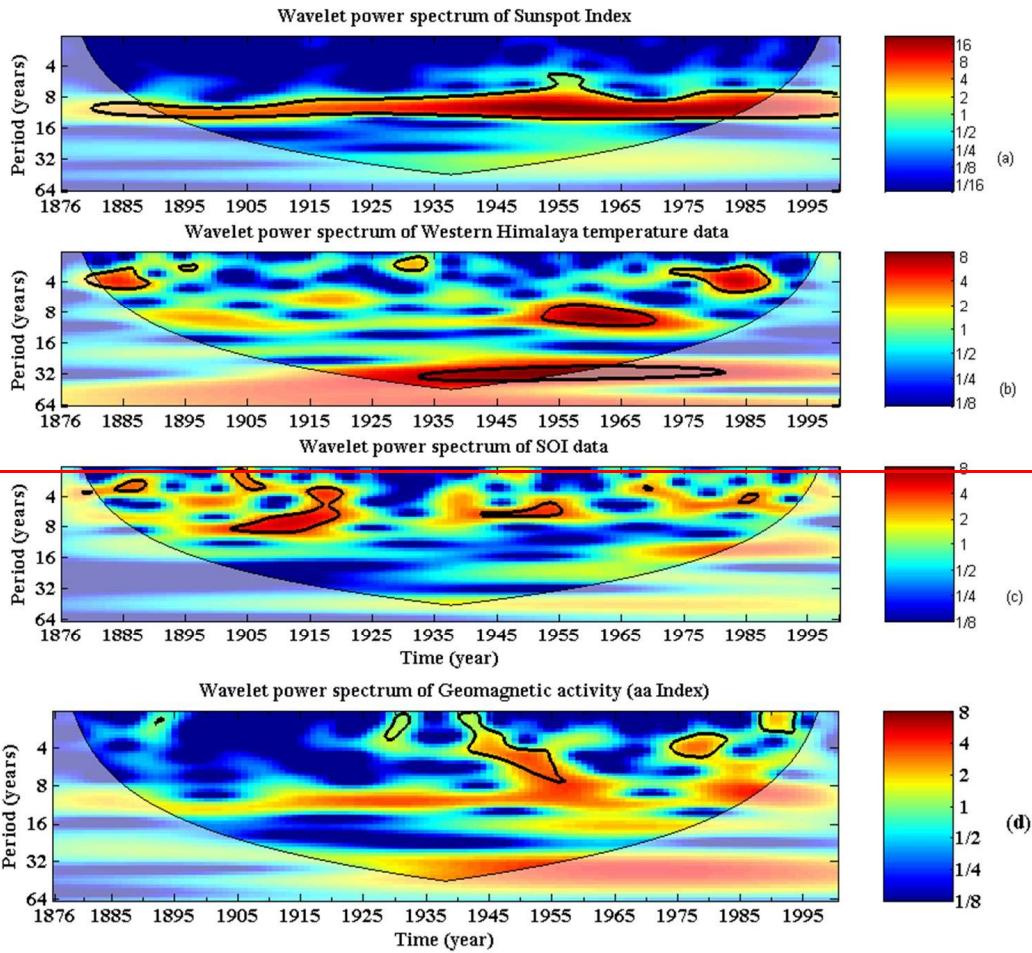
656

657

Figure 3. Power spectra of the first four principal component (PCs) (PC1-4 shown in Fig. 2) for all the data sets with their significant periodicities at 124, 11, 4 and 2.8 years are indicated in bold letters.

Formatted: Font: 12 pt, Bold



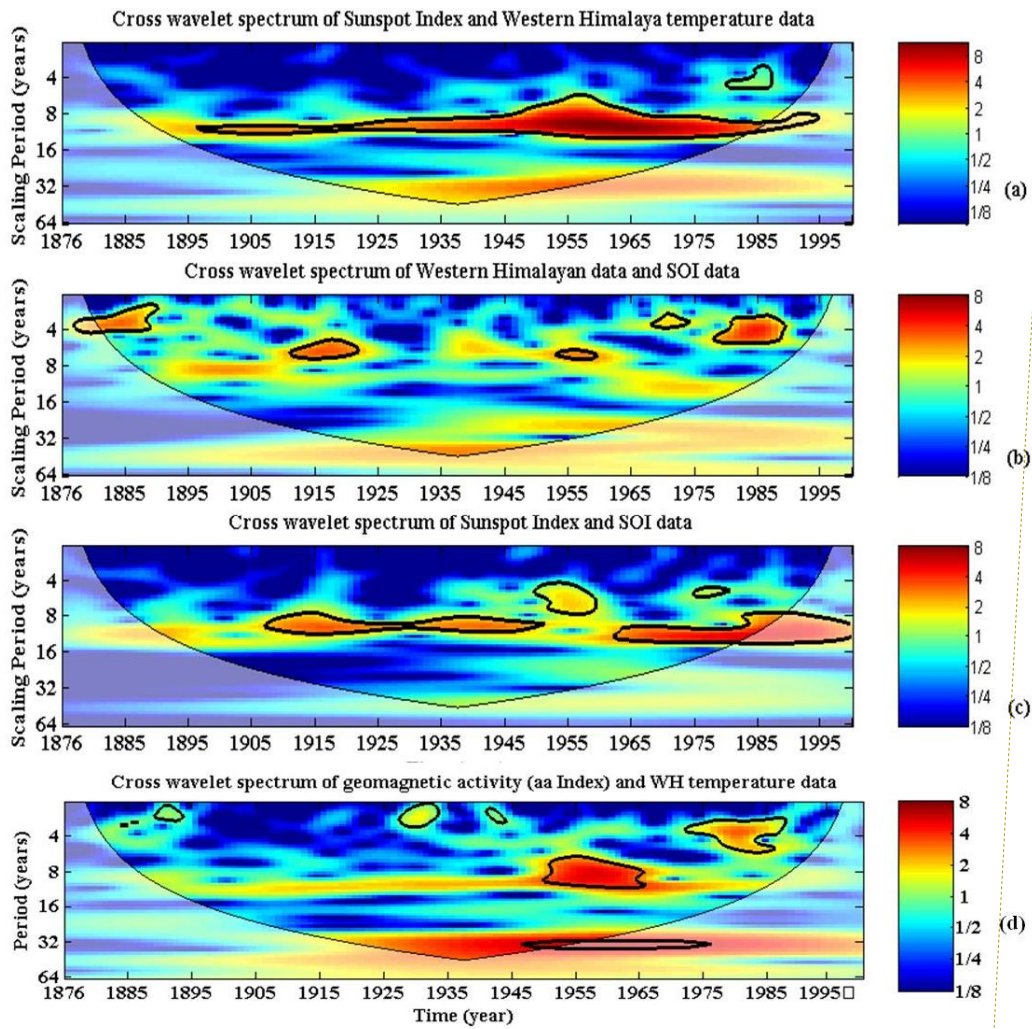


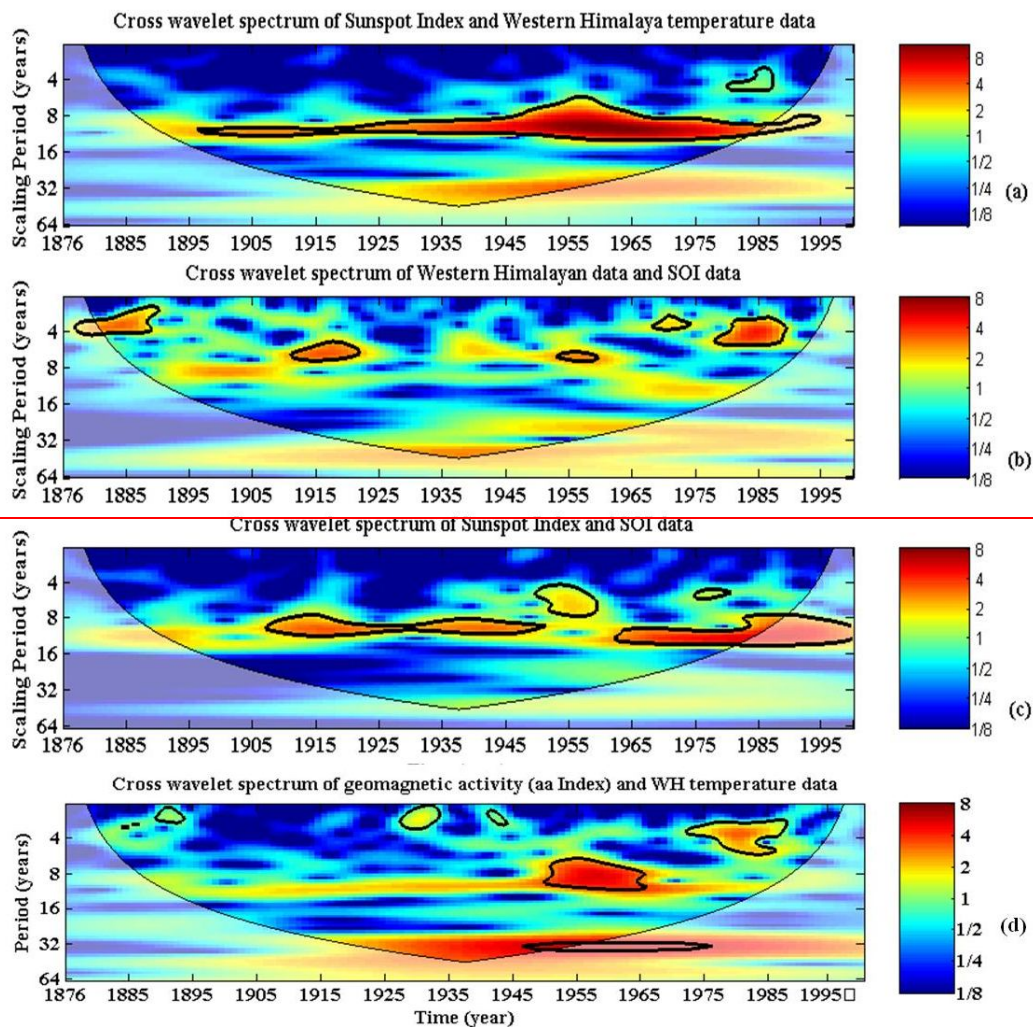
659

660 **Figure 4. Wavelet power spectrum of (a) Sunspot Number (b) Western Himalaya temperature**
 661 **data (c) Southern Oscillation Index (SOI) and (d) Geomagnetic activity (aa Indices) with cone**
 662 **of influence (lighter shade smooth curve) and black lines indicate significant power on 95%**
 663 **level compared to red noise based on first order auto-regressive (AR(1)) coefficient. The**
 664 **legend on right indicates the cross-wavelet power.**

665

666





668

669

670

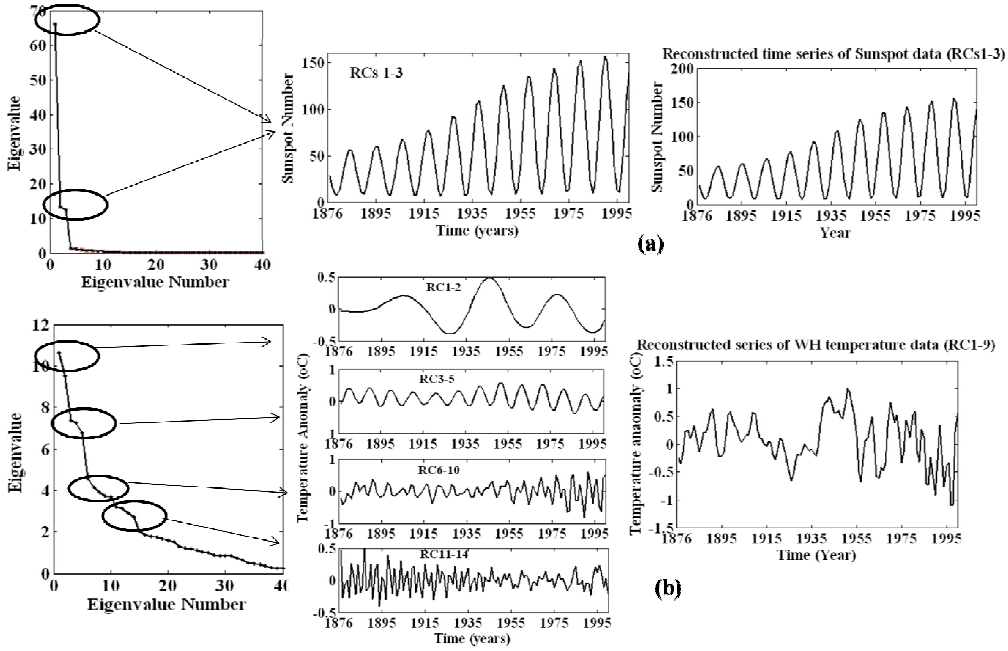
671

672

673

674

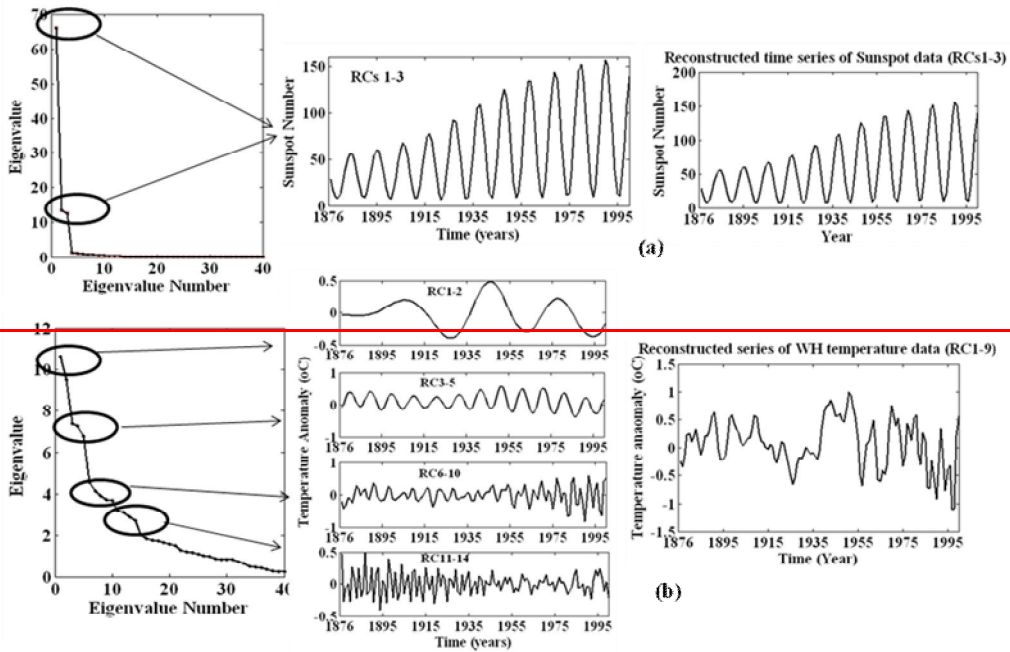
Figure 5. Cross Wavelet spectrum between (a) Sunspot number-Western Himalayan data (b) Western Himalayan-Southern Oscillation Index (c) Sunspot number- Southern Oscillation Index and (d) Geomagnetic: aa indices-Western Himalayan data with cone of influence (lighter shade smooth curve) and black lines indicate significant power on 95% level compared to red noise based on AR(1) coefficient. The legend on right indicates the cross-wavelet power.



675

676

677



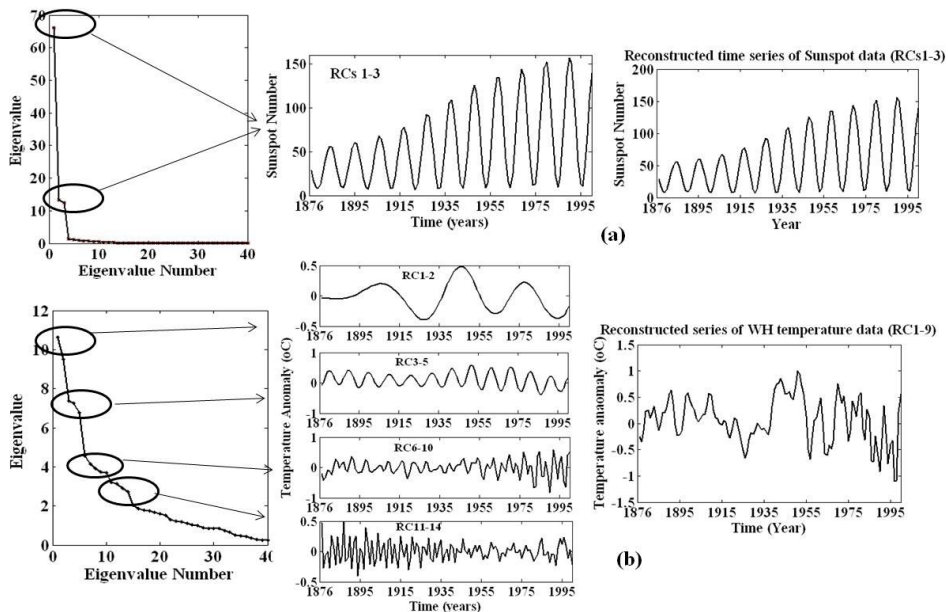
678

679

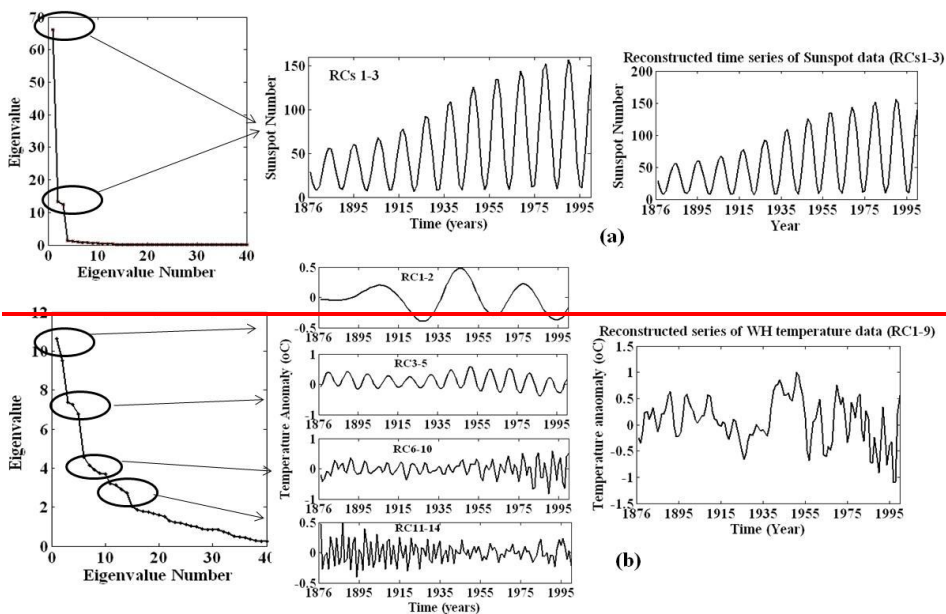
680

Figure 6. Singular spectra with its SSA decomposed components & its reconstructed time series for (a) Sunspot Number and (b) Western Himalaya temperature data.

681

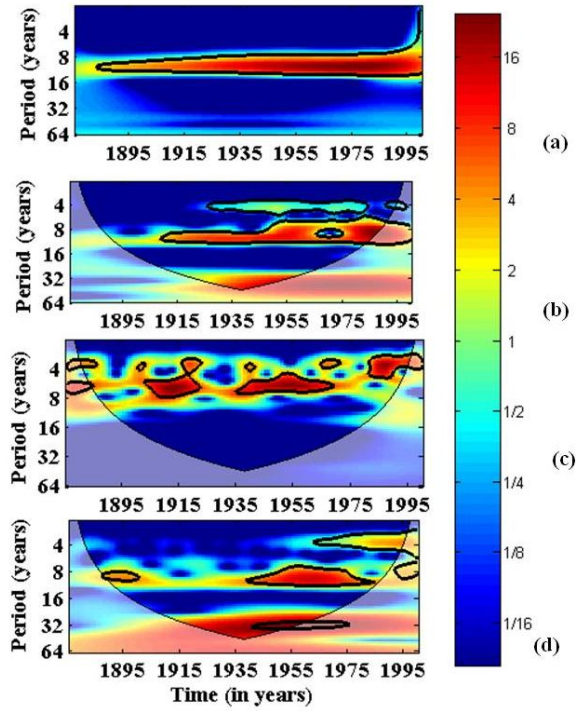
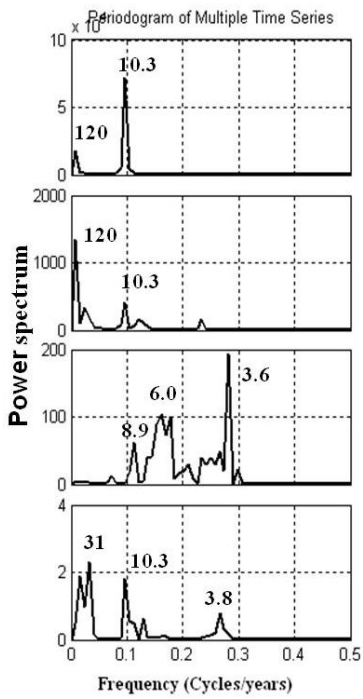


682

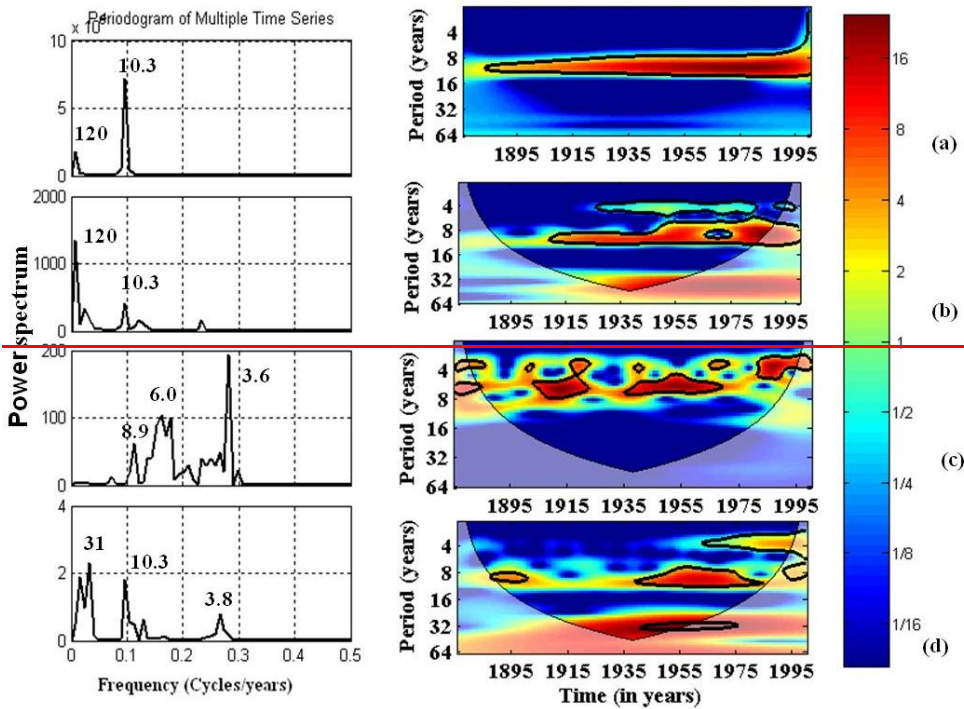


683

684 **Figure 7. Singular spectra with its SSA decomposed components & its reconstructed time**
685 **series for (c) SOI and (d) Geomagnetic activity (aa Indices).**



Formatted: Font: 12 pt, Bold



687

688

689

690

691

692

693

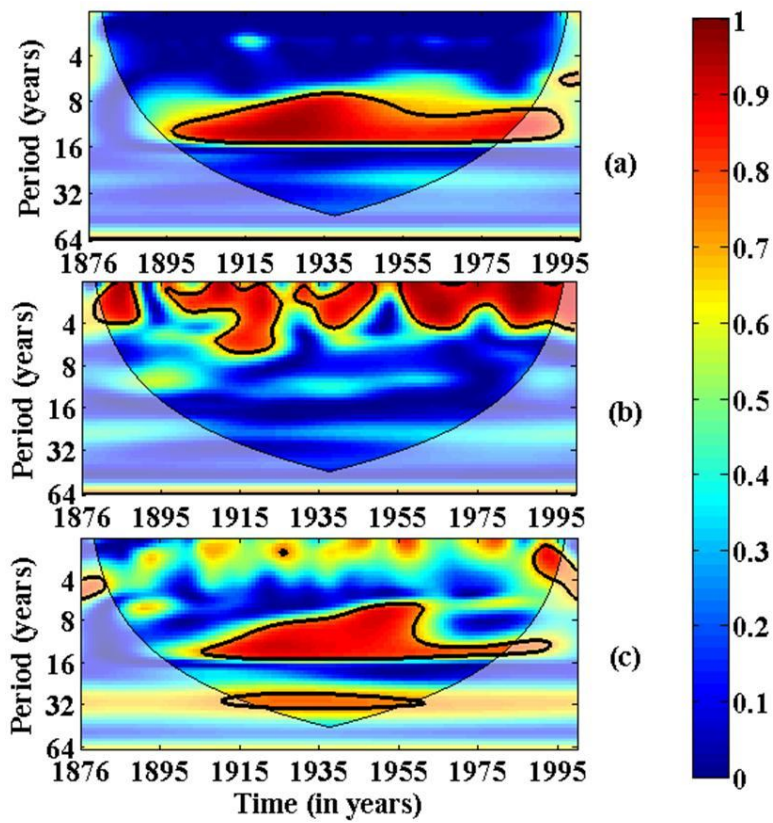
694

695

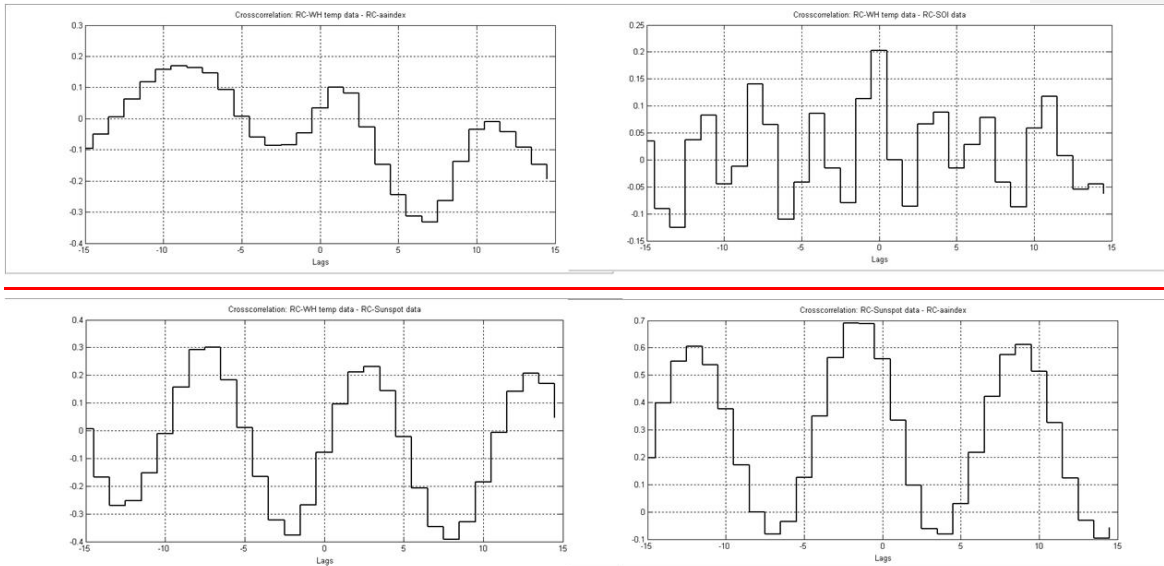
696

697

Figure 8. Power spectrum and Wavelet power spectrum of SSA reconstructed (a) Sunspot data (b) Geomagnetic Indices (aa index) (c) SOI index and (d) the Western Himalayas temperature data with cone of influence (lighter shade smooth curve) and black lines indicate significant power on 95% level compared to red noise based on AR(1) coefficient. The legend on right indicates the cross-wavelet power.



Formatted: Font: 12 pt, Bold



699

700 **Figure 9. Squared wavelet coherence plotted for the SSA reconstructed time series between**
 701 **(a) WH-SSN (b) WH-SOI and (c) WH-aa index with cone of influence (lighter shade smooth**
 702 **curve) and black lines indicate significant power on 95% level compared to red noise based on**
 703 **AR(1) coefficient.**

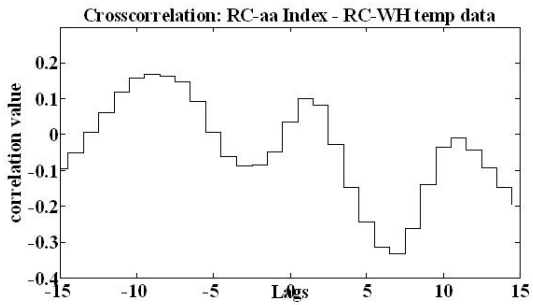
704

705

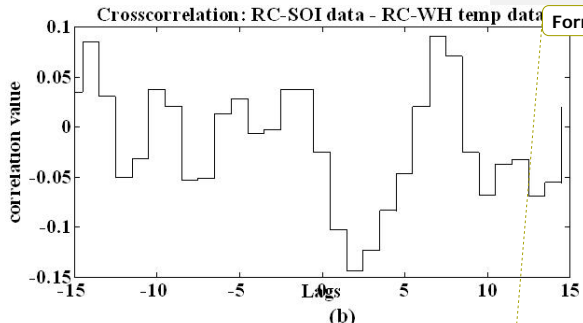
706

707

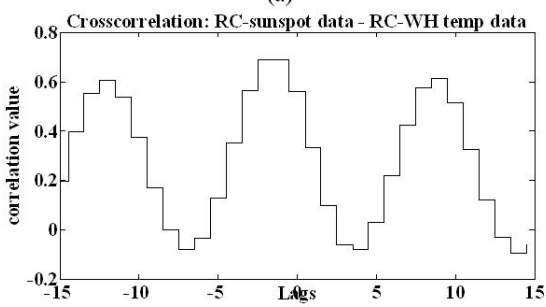
708



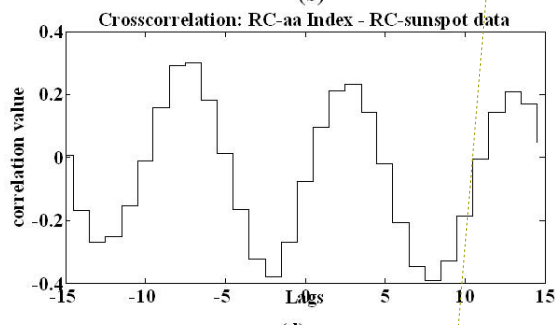
(a)



(b)



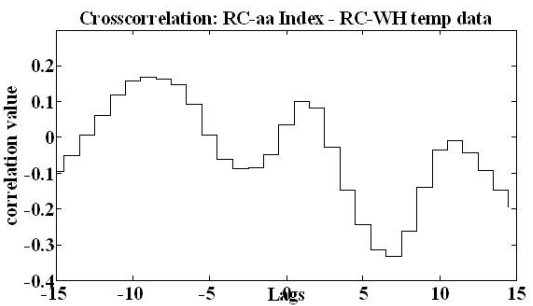
(c)



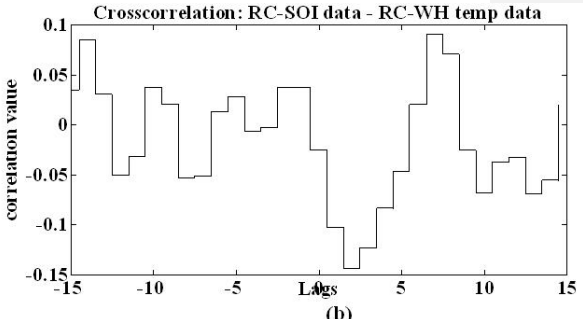
(d)

Formatted: Font: 12 pt

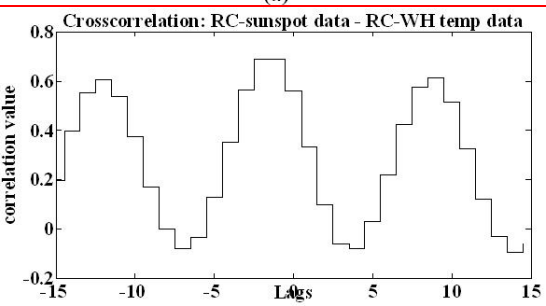
709



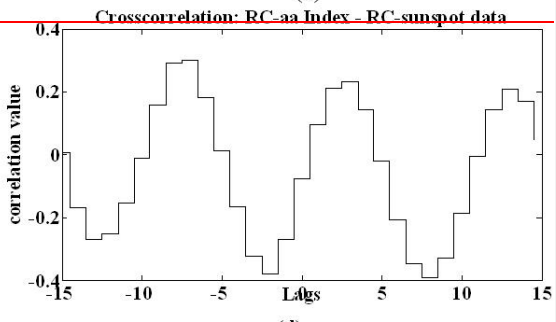
(a)



(b)



(c)



(d)

710

711 **Figure 10. Cross-correlation of SSA reconstructed time series of (a) aa Index-Western**
712 **Himalayan (WH) temperature data; (b) SOI-WH temperature data; (c) sunspot –WH data and**
713 **(d) aa Index-sunspot data.**

714

715

716

